TETRA TECH

TECHNICAL MEMO

ISSUED FOR REVIEW

To:	Mark Adams, Envirowest Consultants	**Date:**	May 22, 2018
c:		**Memo No.:**	001
From:	Albert Leung, Jim Stronach	**File:**	TRN.WTRM03070
Subject:	Interim Progress Report – Modelling of Fugitive Sediment Release during Dredgeate Placement		

This 'Issued for Review' document is provided solely for the purpose of client review and presents our interim findings and recommendations to date. Our usable findings and recommendations are provided only through an 'Issued for Use' document, which will be issued subsequent to this review. Final design should not be undertaken based on the interim recommendations made herein. Once our report is issued for use, the 'Issued for Review' document should be either returned to Tetra Tech or destroyed.

1.0 INTRODUCTION

Tetra Tech Canada Inc. (Tetra Tech) has been retained by Pacific Coast Terminals (PCT) to conduct a numerical modelling study, in support of PCT's permitting process with Environment Canada and other relevant agencies, to investigate the fate of the fugitive sediment released during the proposed dredging operation in the waters off of the Pacific Coast Terminals in Port Moody Arm. This report addresses the combined (sand, silt and clay) total suspended solid (TSS) concentration for the top 3 m at the project site, including consideration of alternative mitigation at a distance of 300 m away from the dispersal site. Since the sediment plume generated by the dispersal operation is not static and varies with tidal stages and local changes in circulation patterns in Port Moody, among other factors, a snapshot of the plume at a point in time is not sufficient to represent the behaviour of the sediment plume and the resulting TSS concentration in the area. A statistical analysis, therefore, is undertaken to determine a more quantitative picture of the variability of TSS concentration over time.

A propriety numerical hydrodynamic model, H3D, is used for this model study. With the information on the properties of the sediment, meteorological conditions, tidal fluctuation, freshwater inflow from rivers and operation schedule and discharge capacity of the diffuser, H3D will track the fate and transport of the TSS during the operation and provide spatial and temporal patterns of the suspended solids in the water column.

2.0 METHODOLOGY

2.1 Numerical Model

A detailed technical description of H3D is attached in Appendix A.

The primary numerical model employed in this study is a 25-m resolution three-dimension numerical model encompassing Burrard Inlet from just east of Second Narrows to the Port Moody Arm. This model is the highest resolution model in a series of numerical models extending from the Pacific Ocean to the east end of Port Moody Arm:

- Coarse Resolution: 1-km resolution shelf model extending from the mouth of Juan de Fuca Strait to the southern end of Texada Island and the terminus of Indian Arm. The model is driven by tidal constituents

Tetra Tech Canada Inc.
Suite 1000 – 10th Floor, 885 Dunsmuir Street
Vancouver, BC V6C 1N5 CANADA
Tel 604.685.0275 Fax 604.684.6241

and monthly climatology at its boundaries with hourly wind fields and daily river inflows at 13 significant rivers based on observed data in 2012.

- Mid-Resolution: 125-m resolution Burrard Inlet model extending from the entrance to English Bay to the terminus of Indian Arm and Port Moody Arm. The model is driven by water level, temperature and salinity data from the coarse resolution model, with observed hourly wind fields and daily river inflows in 2012.
- High Resolution: 25-m resolution Burrard Inlet model extending from just west of the Second Narrows Bridge to the east end of Port Moody Arm, driven by water level, temperature and salinity data at two open boundaries from the mid-resolution model (Figure 2.1), with observed hourly wind fields and daily river inflows in 2012.

Within the modeling chain, all major rivers in the Salish Sea are included, with Lynne Creek, the Seymour River and the Capilano River feeding directly in the high resolution Burrard Inlet model. Wind fields are interpolated from measured winds at buoys and meteorological stations around coastal British Columbia, with winds for the high resolution Burrard Inlet model based on a dedicated CALMET wind model.

Figure 2.1 shows the location of the project site at PCT and the extent of the 25-m fine resolution Burrard Inlet model.

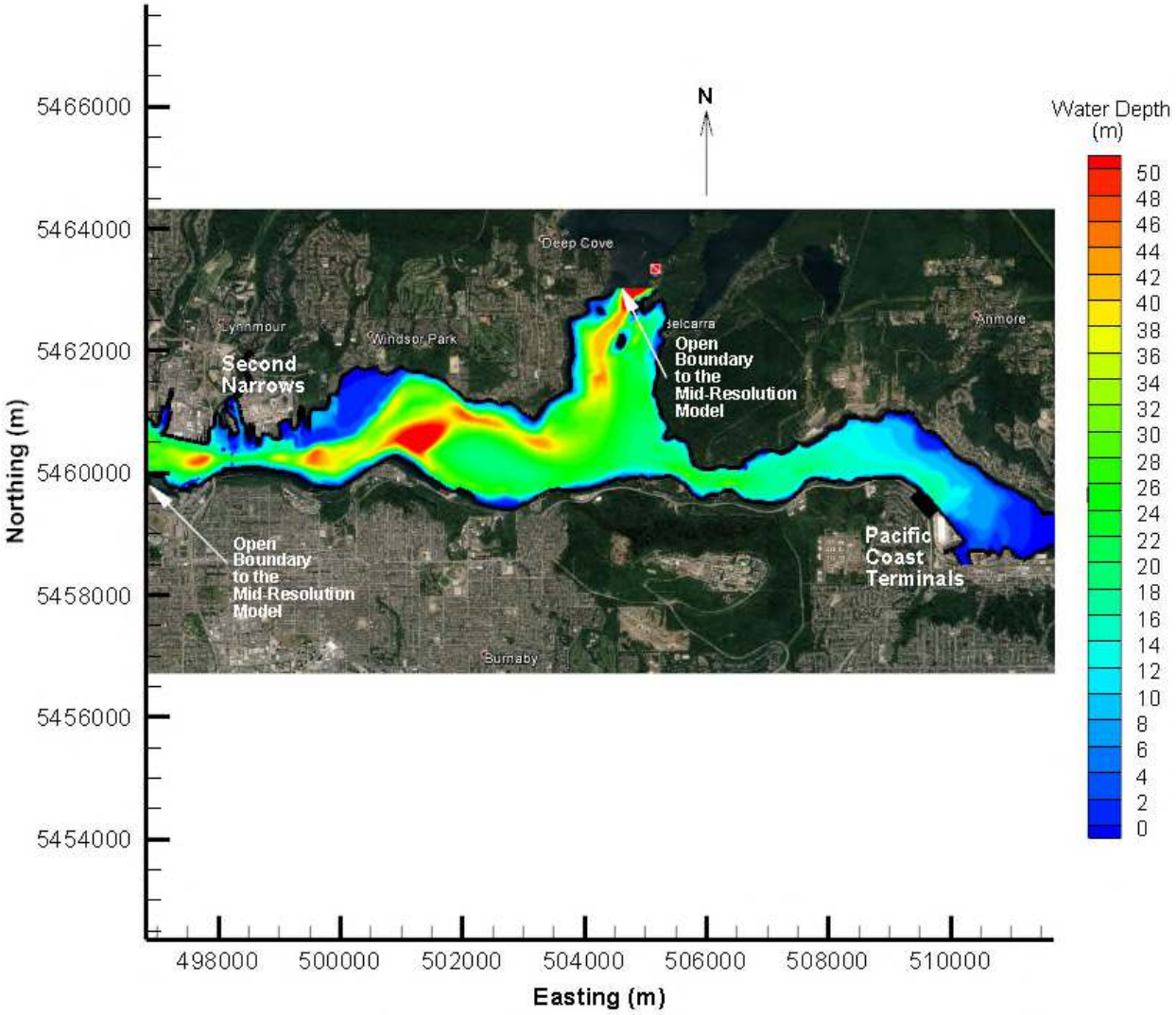

Figure 2.1 Location of the Project Site and Domain of the Fine Resolution Model

2.2 Fugitive Sediment Plume Tracking

In order to quantify the dispersion of fugitive sediments, the total suspended solids (TSS) content of the fugitive sediment plume is tracked as sediments are released over a simulated dredging program as described in Section 3. The concentration of the TSS within the domain of the fine-resolution model is extracted and reported. The TSS concentration, averaged over the top 3 m of the water column, at the project site, especially at a distance 300 m away from the dredgeate disposal area, is the main focus of this report. The modelled concentration will be compared to the 24-hour exposure criterion value of 25 mg/L (equivalent to 8 NTU) as stated in the CCME Water Quality Guidelines for Protection of Aquatic Life.

3.0 DREDGE OPERATION

This section briefly describes the parameters of the dredge/discharge operation, which is largely based on the information provided by John Halmarick of Fraser River Pile and Dredge (FRPD) and Mark Adams of Envirowest.

3.1 Disposal Volume

The total volume of the proposed dredge prism is approximately 550,000 m^3. Based on the moisture content (66.4%) of the four sediment samples that were analyzed by ALS Environmental at the proposed dredge location in August 2017 (ALS, 2017), the void ratio of the in-situ sediment on the bed is approximately 1.76. As such, the total volume of solids dredged is approximately 201,213 m^3.

3.2 Disposal Location

The dredgeate will be placed into two containment basins: 1) the new main containment basin and 2) the existing containment basin. The main basin would be bounded by the newly constructed west and north berms, the existing berm to the east and the 4.5 m chart datum bathymetric contour to the south. The existing containment is bounded by the existing berm to the west and 4.5 m chart datum bathymetric contour to the east. Figure 3.1 illustrates the layout of the containment basins for the dredgeate. The figure also indicates the alignment of the new and existing berms, as well as the 300-m equi-distance demarcation lines drawn 300 m nominally away from the disposal area. The disposal area consists of both the new and existing containment basins.

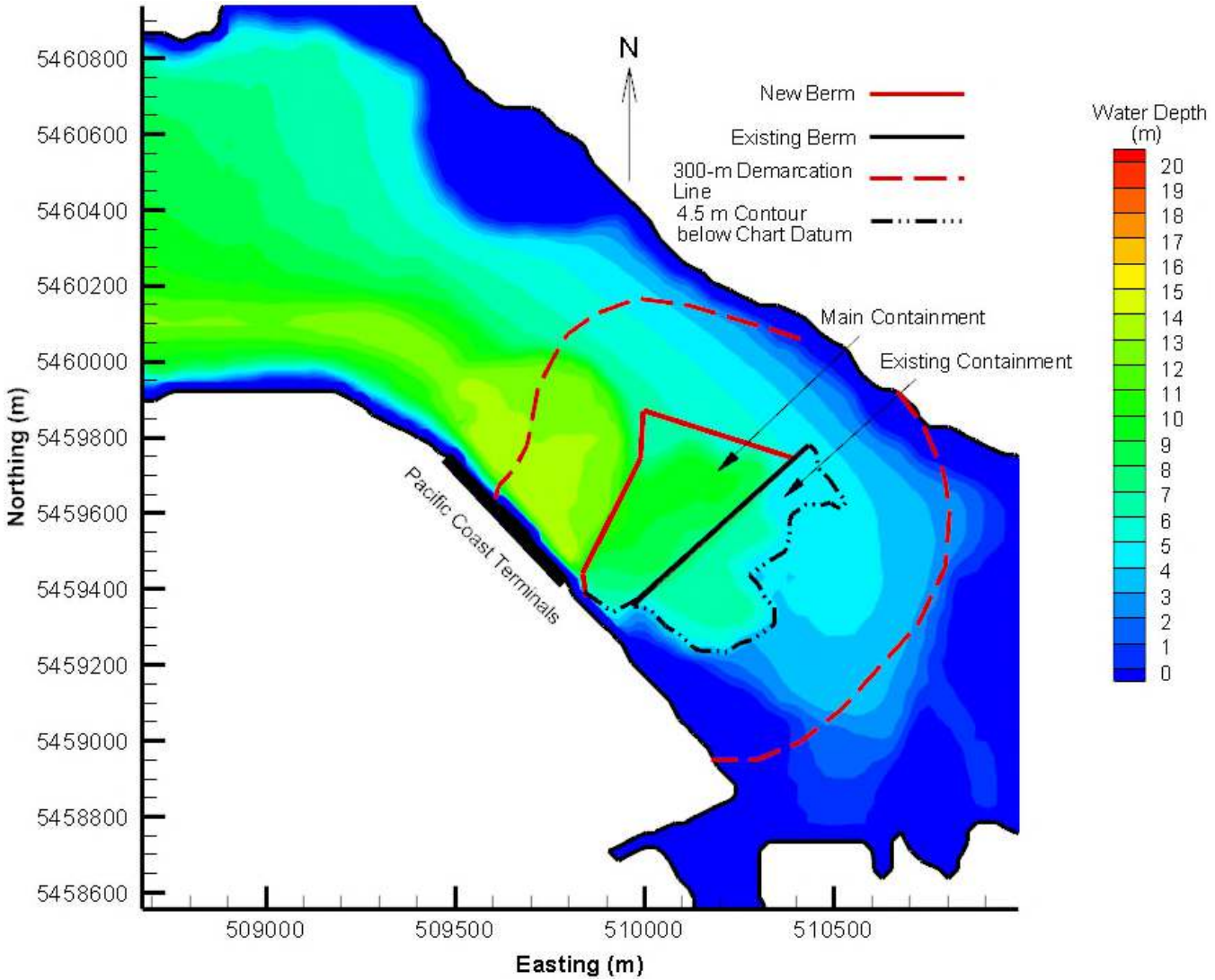

Figure 3.1 Layout of the Containment Basins and Existing Bathymetry in Port Moody Arm

3.3 Operation Period and Dredge Cycle

The dredging and dispersal operation is projected to occur between mid-September to late November or early December 2019, taking approximately 8-10 weeks to complete. For the purposes of modelling, two different dredgers will be utilized for the dredge operation: the 309 and the Columbia. While the Columbia dredger will be deployed most of the time during the operation period, the 309 dredger will only be in operation for approximately 10 days. For this modelling study, the Columbia is assumed to operate between October 5th and December 2nd; the operation with the 309 dredger will last for approximate 10 days in two separate models, either in the early period when the containments are nearly empty or in the late period when the containments are nearly full. Of the solid volume of 199,400 m^3 (corresponding to 550,000 m^3 dredge prism volume presented in Section 2.1) that is to be taken out of the proposed dredge prism, 163,145 m^3 of solid will be taken out by the Columbia dredger and 36,255 m^3 of solid will be dredged by the 309 dredger.

The Columbia dredger will operate with a duty cycle of 60%: 60% of the time, dredgeate will be discharged into the containment basins and 40% of the time the Columbia will not be discharging dredgeate. For this study, it is

assumed that the Columbia operation has a 5-hour cycle, in which 3 hours are spent discharging the dredgeate and 2 hours spent not discharging. The 309 dredger will have a dredge/discharge cycle of 2.5 hours, of which 2 hours are taken for loading and traversing between the load site and disposal site, and 0.5 hours taken for dispersing the dredgeate. While the dredge operation associated with both dredgers will be continuous, the two dredgers will not operate simultaneously and thus the sediment released by the two dredgers has been modelled independently with no interference and additive effects from one dredge operation on the other.

3.4 Silt Curtain

A silt curtain is proposed to be used to help control the spatial extent of any plumes arising from the placement of the dredgeate. The silt curtain will be suspended from the water surface to 3 m deep surrounding the release point. The curtain is 80 m long and will enclose an approximate 20 m by 20 m area at the same horizontal location of the discharge diffuser which will reduce the discharge velocity of sediment and water from the Columbia.

3.5 Diffuser Discharge

The operation plan is to have the dredegate transported by a pipe and released within the containment basins at the terminus near the bed. Tetra Tech recommends that the diffuser terminus be moved regularly, from deep waters to shallow waters, in order to ensure the even filling of the dredgeate in the containment basins. The plan is to first discharge the dredgeate in the main basin until it is filled up, after which the diffuser will be moved to and commence discharging in the existing basin. Figure 3.2 indicates the proposed route of the diffuser movement during the operation.

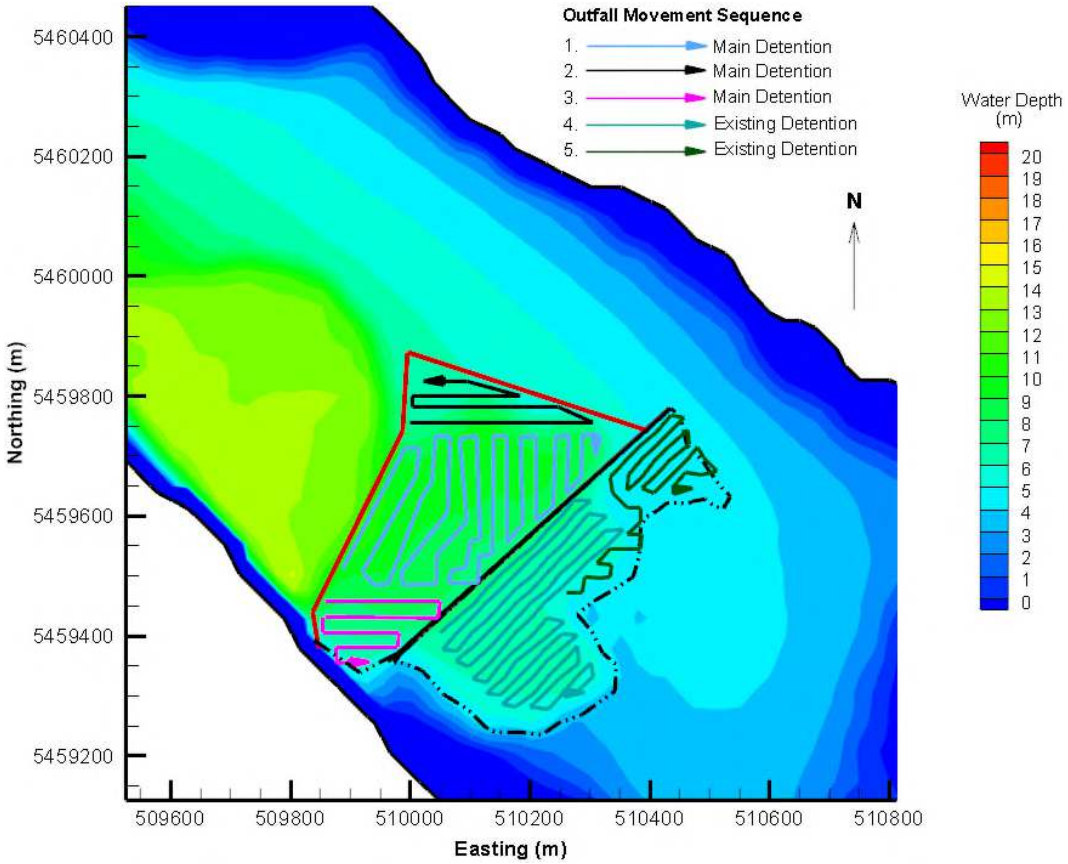

Figure 3.2 Diffuser Movement Sequence

4.0 SEDIMENT CHARACTERISTICS

ALS Environmental undertook a particle size analysis of the sediments that were collected in August 2017 within the proposed dredge cut. The sediments were mainly composed of finer material (57% for silt and 29% for clay) with a significantly smaller portion for sand (14%).

The sinking rate of these sediments often depends on the particle size, and it is the case for this project for sand and silt whose sinking velocities were derived from Stokes' law. However, flocculation is a well known phenomenon, especially for finer material such as clay, in a brackish environment where freshwater mixes with saltwater, leading to a higher sinking velocity. Tarbotton *et al.* (1999) undertook a settling column test for the sediment collected at the PCT site prior to the most recent dredging operation in the area. Although the authors were not particularly investigating the effects of flocculation, they found that, during the initial settling period, the edge of the turbidity layer sunk at 0.11 m/hr or 0.00003 m/s. We postulate that the edge of the turbidity layer is comprised of mostly clay material and the observed sinking velocity is faster than what would be predicted by Stokes' Law for clay material likely due to effects from flocculation.

Table 4.1 summarizes the sediment composition of the dredgeate and the sinking velocity of these sediments that are implemented in this model study.

Table 4.1 Sinking Velocity and Sediment Composition of the Dredgeate at the PCT Site

Sediment Composition*	
Gravel	0%
Sand	14%
Silt	57%
Clay	29%
Sinking Velocity	
Gravel	N/A
Sand	0.00980 m/s
Silt	0.00016 m/s
Clay	0.00003 m/s**

* based on ALS' particle size analysis report (2017)

** based on the settling column test conducted by Tarbotton *et al.* (1999)

Because of the high silt and clay fractions in the sediment, specialized dredgeate placement practices are contemplated (Mastbergen *et al.*, 2004). Various methods of discharging the dredgeate are described in Mastbergen *et al.*, (2004), the common goal being to ensure that the dredgeate enters the disposal area with a relatively slow horizontal velocity, directed radially from the feed pipe. This approach allows the dredgeate to form a density current, which moves the sediment away from the release point. Furthermore, the density contrast between the density current and the overlying Port Moody Arm brackish water will suppress the vertical mixing, further ensuring the trapping of the dredgeate near the bottom. For the modelling discussed here, the dredgeate is

simply placed in the appropriate model grid cell, at the bottom of the water column, emulating the placement practices discussed above.

5.0 MODEL RESULTS

As the containment basin fills up, the water depth in the basin becomes shallower, as does the discharge depth of the dredgeate. As a result, the behaviour of the anticipated fugitive sediment will likely change, when comparing the initial and late stages of the disposal operation. AS such, 2 separate time windows during the operation period, categorized by the various filling stages of the basins, will be considered: 1) the early period when both containment basins are nearly empty (bathymetry similar to the existing), and 2) the late period when both containment basins are nearly full (approaching elevation 4.5 m below chart datum). The two tie period will likely reprsent

These time windows are intended to provide insight into predictive transitional operational conditions as the containment basins are filled. Nonetheless, these time windows capture a typical set of environmental conditions and physical settings that will be encountered.

Since the operation timing for both the Columbia and 309 dredgers are uncertain at the time of writing of this report; in other words, the Columbia and 309 could operate in any part of the operation timeline. For this study, 4 separate modelling scenarios are therefore considered:

1- Operation of the Columbia dredger in the early period,

2- Operation of the 309 dredger in the early period

3- Operation of the Columbia dredger in the late period

4- Operation of the 309 dredger in the late period.

These 4 model scenarios does not interfere with each other since the two dredgers will not operate simultaneously.

Figure 5.1 illustrates the early and late stages of the disposal operation, as well as the corresponding water level at Point Atkinson. The information for year 2012 is presented in the figure as 2012

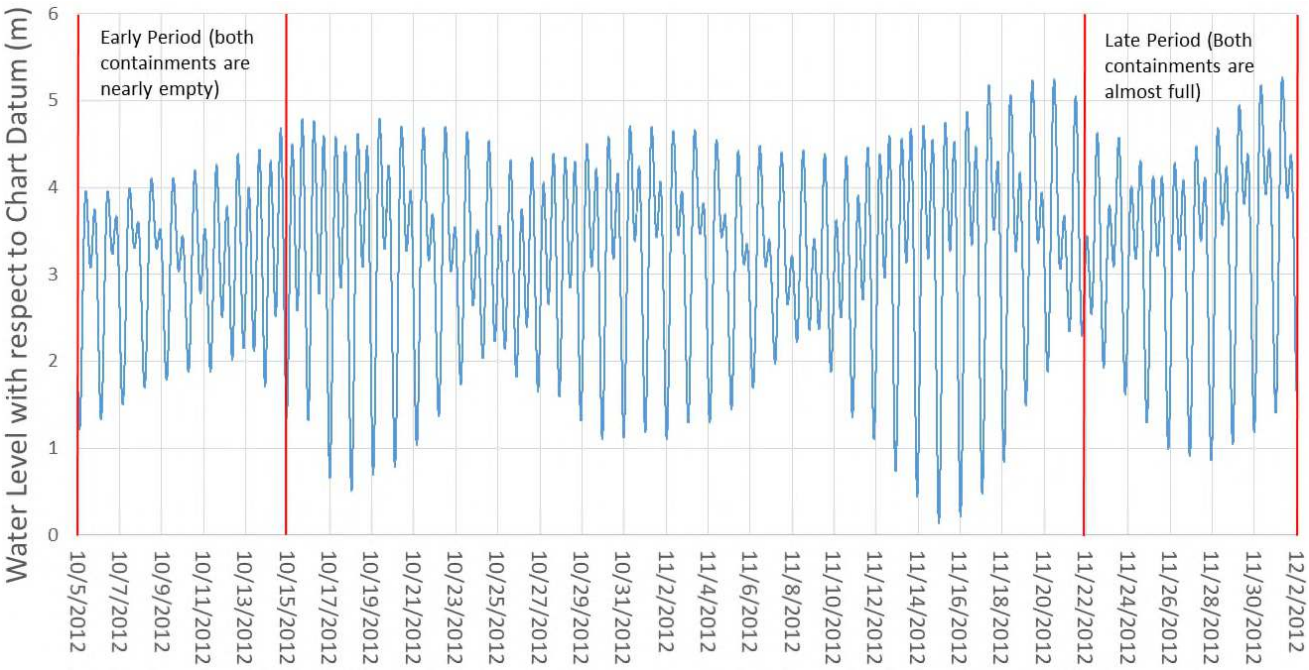

Figure 5.1 Water Level at Point Atkinson and the Two Dredge Operation Time Windows

For operation flexibility, a separate model study was undertaken to investigate the impact of dredgeate dispersal from the 309 dredger if it were to be deployed in either of the early or late periods.

5.1 The Sediment Plume

Snapshots of the plan view and the corresponding cross section views of the combined concentration of total suspended solid (sand + silt + clay), or TSS, averaged over the top 3 m of the water column, were extracted from the model. However, only the snapshots that illustrate the highest TSS concentration in each of the early and late periods are shown and discussed in this section. As such the most conservative 'worst' case conditions are depicted. The two dredgers will not operate simultaneously and thus the sediments released by the two dredgers have been modelled independently with no interference and additive effects from one dredge operation to another.

The water quality criterion for turbidity is 25 mg/L according to the CCME guidelines for the Protection of Aquatic Life.

5.1.1 Early Period – Columbia (Scenario 1)

The snapshot of the TSS concentration, resulting from the Columbia operation, during a flood tide approximately 2 hours before high tide in October, in the top 3-m is shown in plan view in Figure 5.2, and the corresponding sectional TSS profiles along the Northwest-Southeast and Northeast-Southwest lines are shown respectively in Figure 5.3 and Figure 5.4.

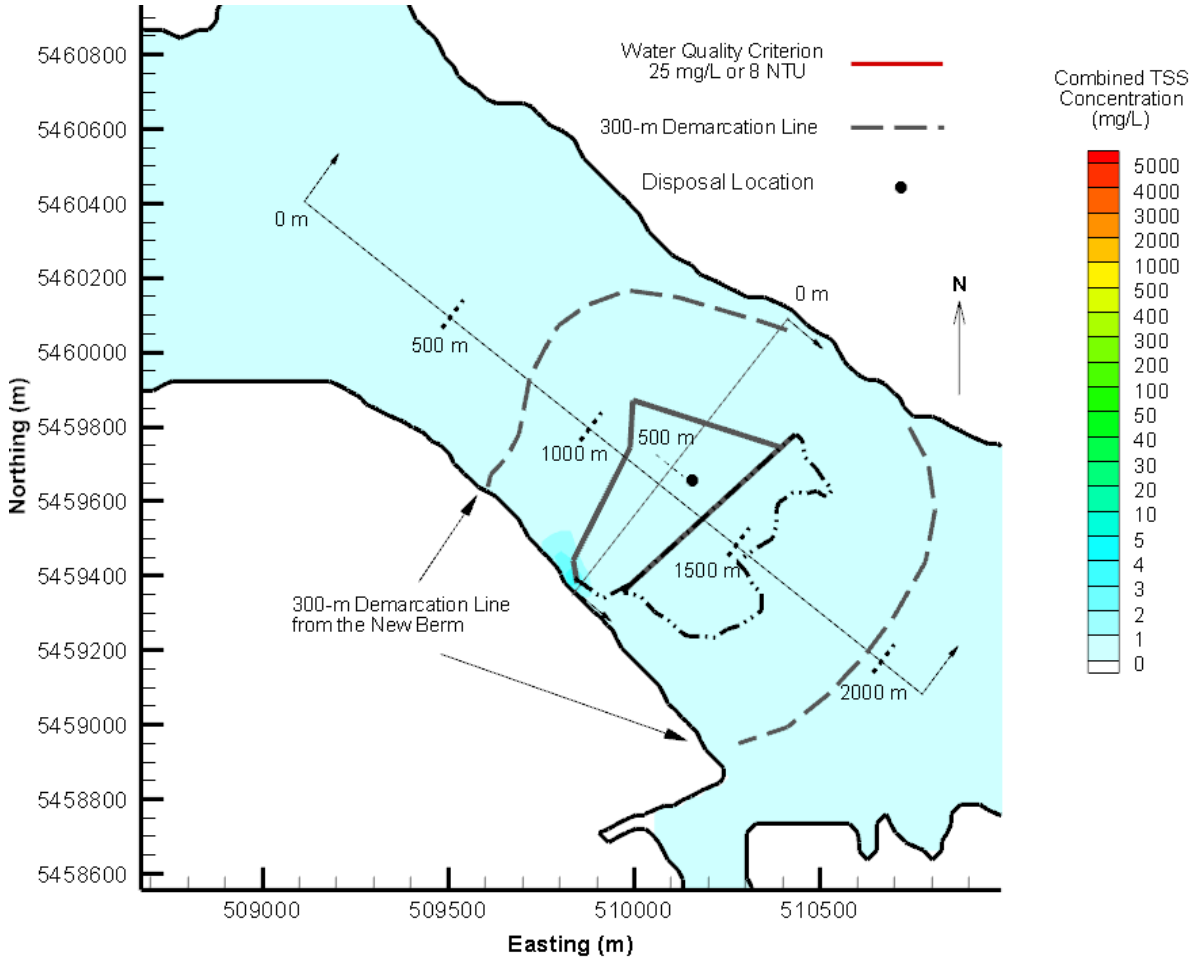

Figure 5.2 Combined TSS Concentration, Averaged between 0 m and 3 m Water Depth in the Early Period (Columbia Dredger) – Flood Tide Approximately 2 hours before High Tide in October

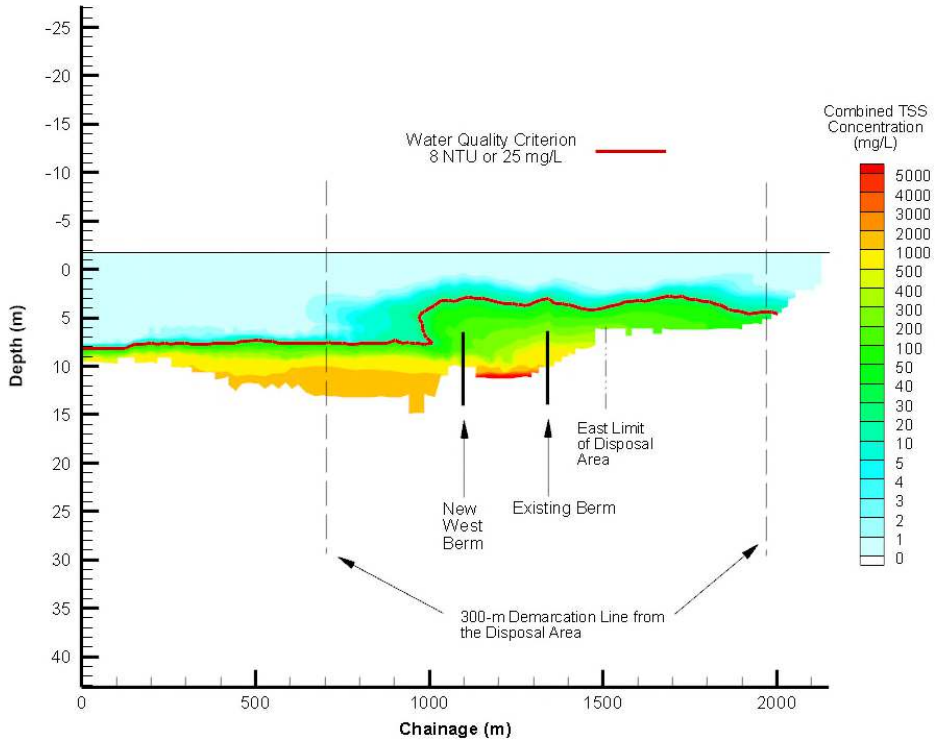

Figure 5.3 Northwest-Southeast Sectional Combined TSS Concentration in the Early Period (Columbia Dredger) – Flood Tide Approximately 2 hours before High Tide in October

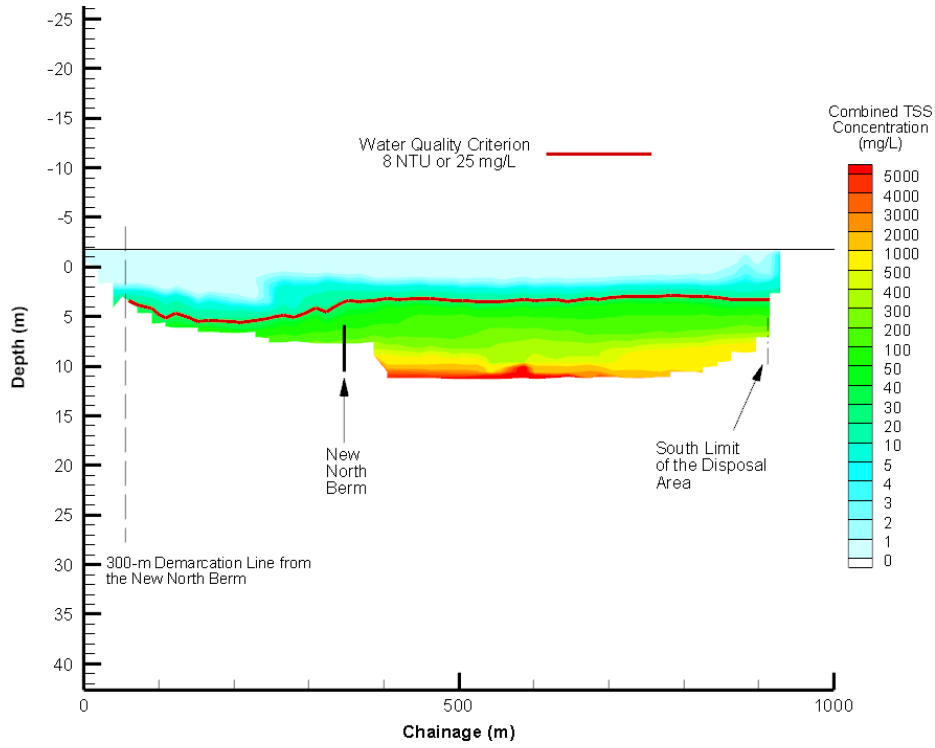

Figure 5.4 Northeast-Southwest Sectional Combined TSS Concentration in the Early Period (Columbia Dredger) – Flood Tide Approximately 2 hours before High Tide in October

The combined TSS concentration indicates a general increasing trend with time as the dredge and disposal operation continues. In general, the 90th percentile combined TSS concentration, averaged over the top 3 m of the water column, stays below 4 mg/L or 1.6 NTU, even towards the end of the 'early' period.

5.1.2 Early Period – 309 (Scenario 2)

The snapshot of the TSS concentration, resulting from the 309 operation, during a flood tide approximately 2 hours before high tide in October, in the top 3-m is shown in plan view in Figure 5.5, and the corresponding sectional TSS profiles along the Northwest-Southeast and Northeast-Southwest lines are shown respectively in Figure 5.6 and Figure 5.7.

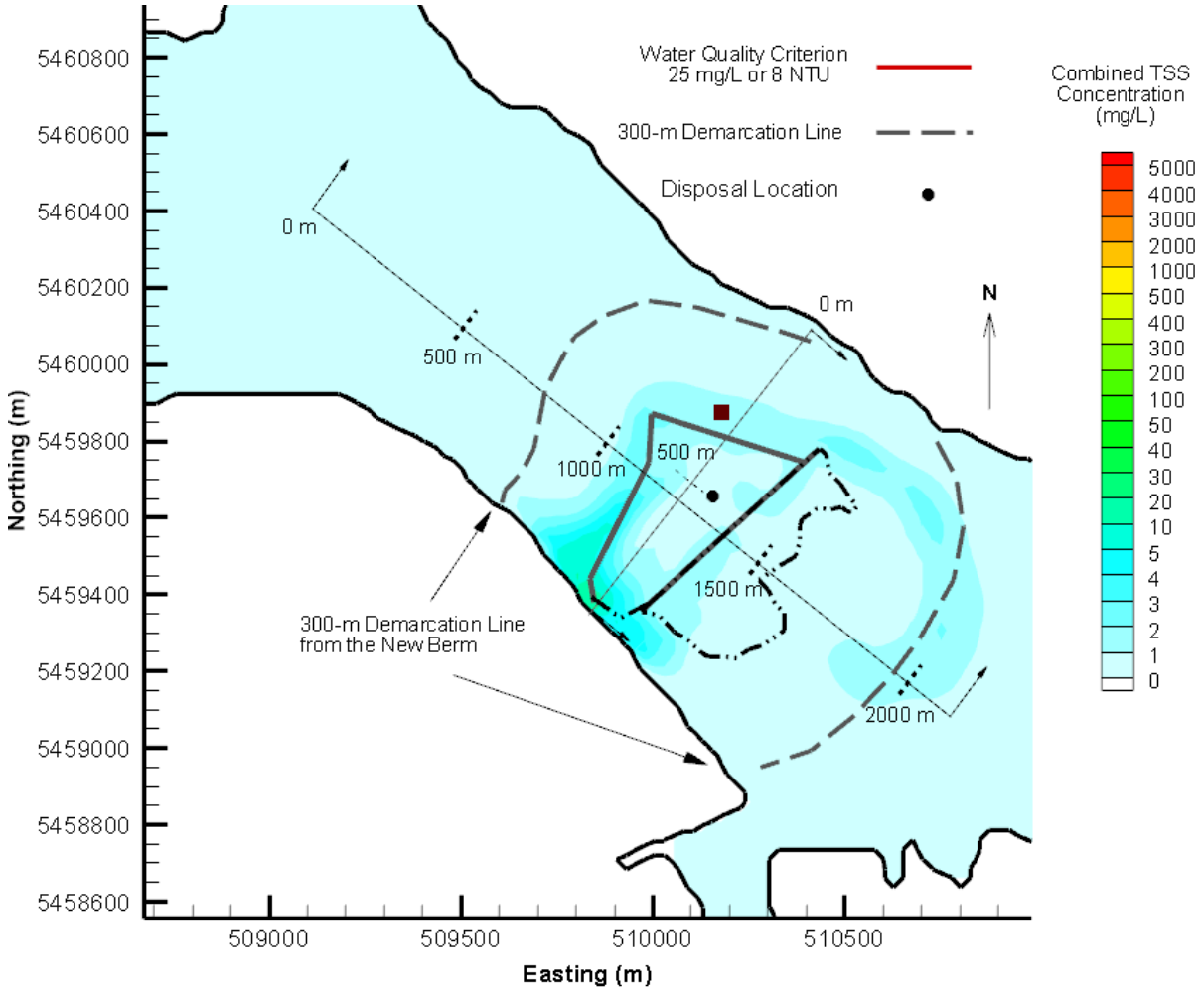

Figure 5.5 Combined TSS Concentration, Averaged between 0 m and 3 m Water Depth in the Early Period (309 Dredger) – Flood Tide Approximately 2 hours before High Tide in October

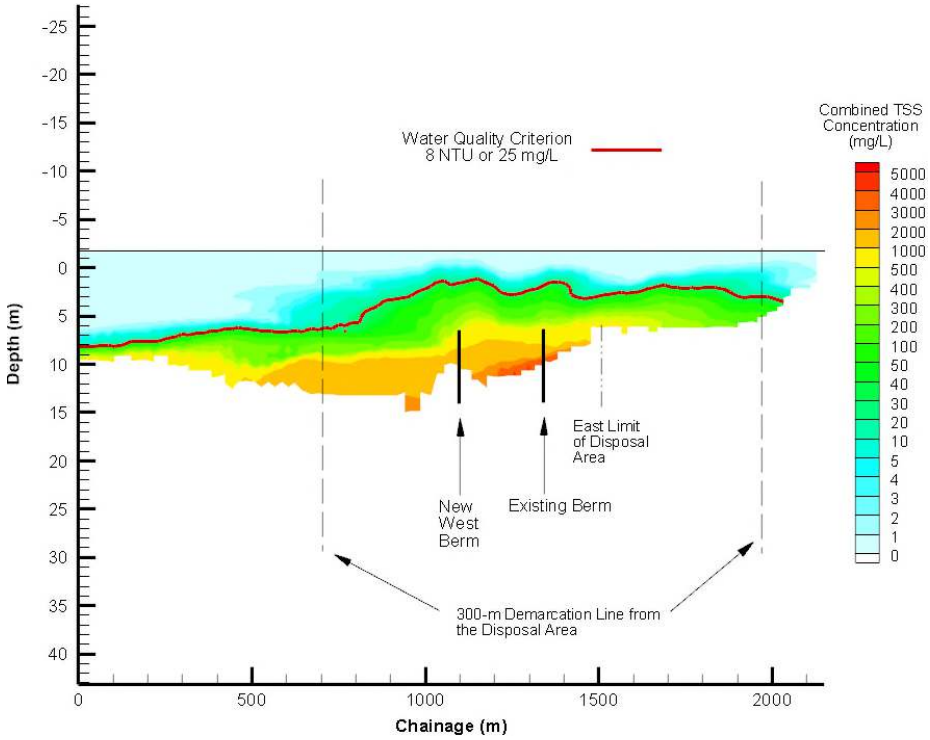

Figure 5.6 Northwest-Southeast Sectional Combined TSS Concentration in the Early Period (309 Dredger) – Flood Tide Approximately 2 hours before High Tide in October

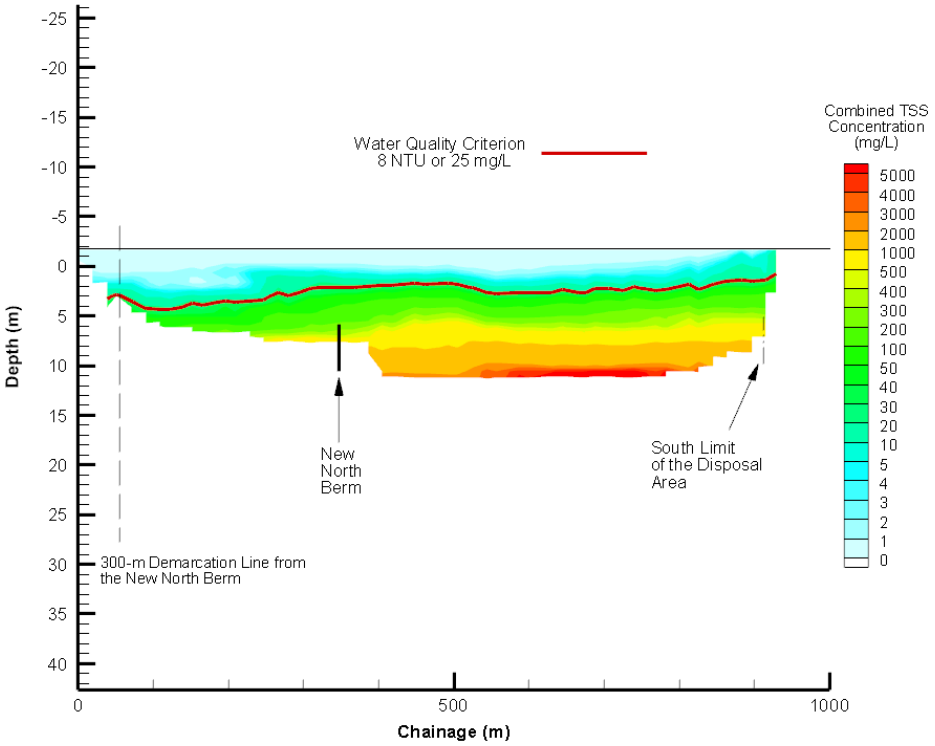

Figure 5.7 Northeast-Southwest Sectional Combined TSS Concentration in the Early Period (309 Dredger) – Flood Tide Approximately 2 hours before High Tide in October

Similar to the Columbia operation, the combined TSS concentration, averaged over the top 3-m, remains lower than the criterion value of 25 mg/L or 8 NTU.

5.1.3 Late Period – Columbia (Scenario 3)

The snapshot of the TSS concentration, resulting from the Columbia operation, during a flood tide approximately 3 hours before high tide in December, in the top 3-m is shown in plan view in Figure 5.8, and the corresponding sectional TSS profiles along the Northwest-Southeast and Northeast-Southwest lines are shown respectively in Figure 5.9 and Figure 5.10.

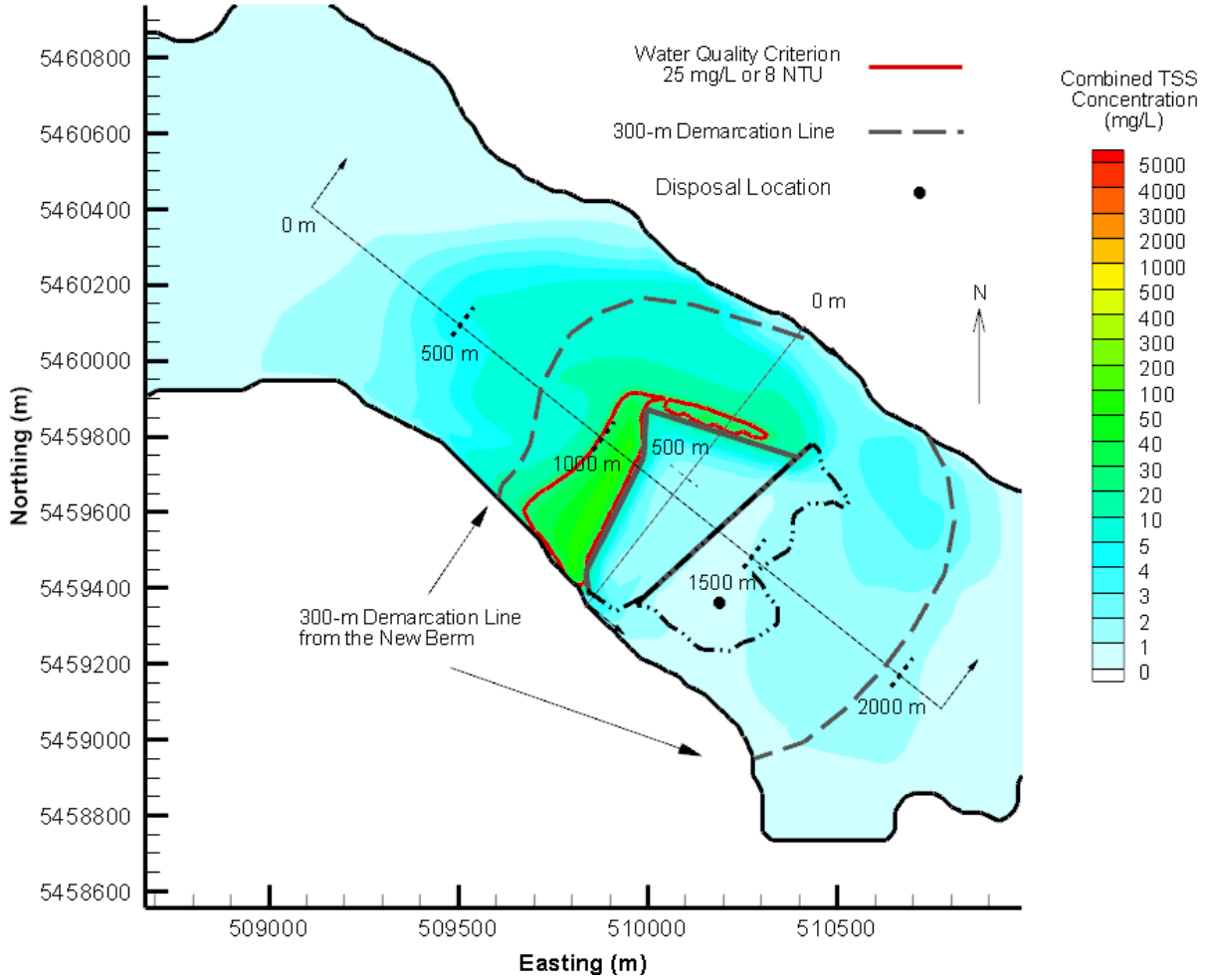

Figure 5.8 Combined TSS Concentration, Averaged between 0 m and 3 m Water Depth in the Late Period (Columbia Dredger) – Flood Tide Approximately 3 hours before High Tide in December

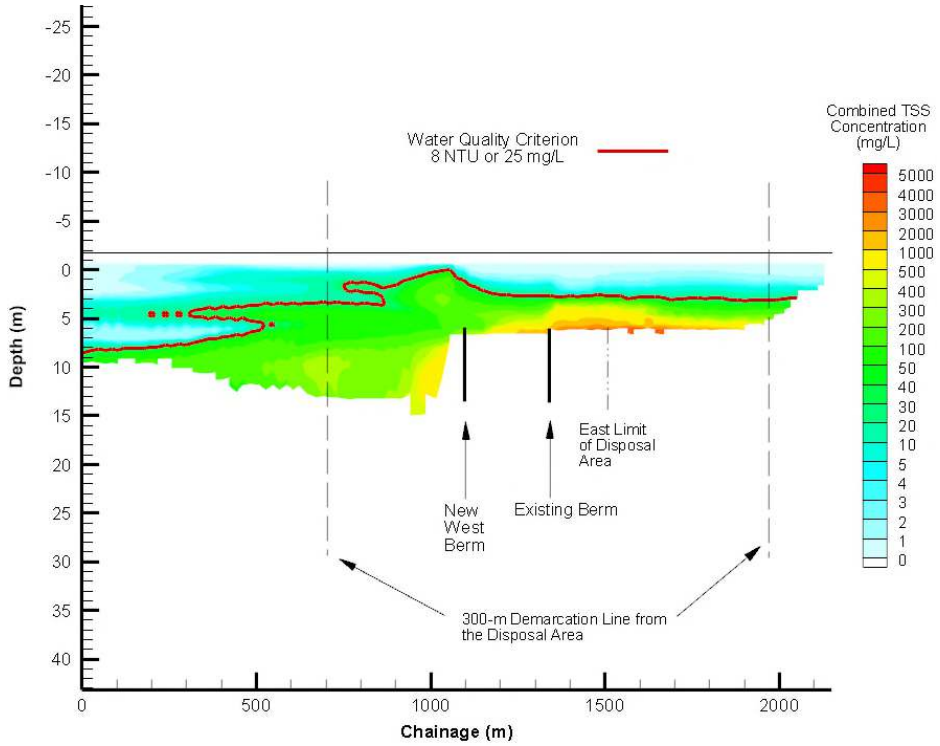

Figure 5.9 Northwest-Southeast Sectional Combined TSS Concentration in the Late Period (Columbia Dredger) – Flood Tide Approximately 3 hours before High Tide in December

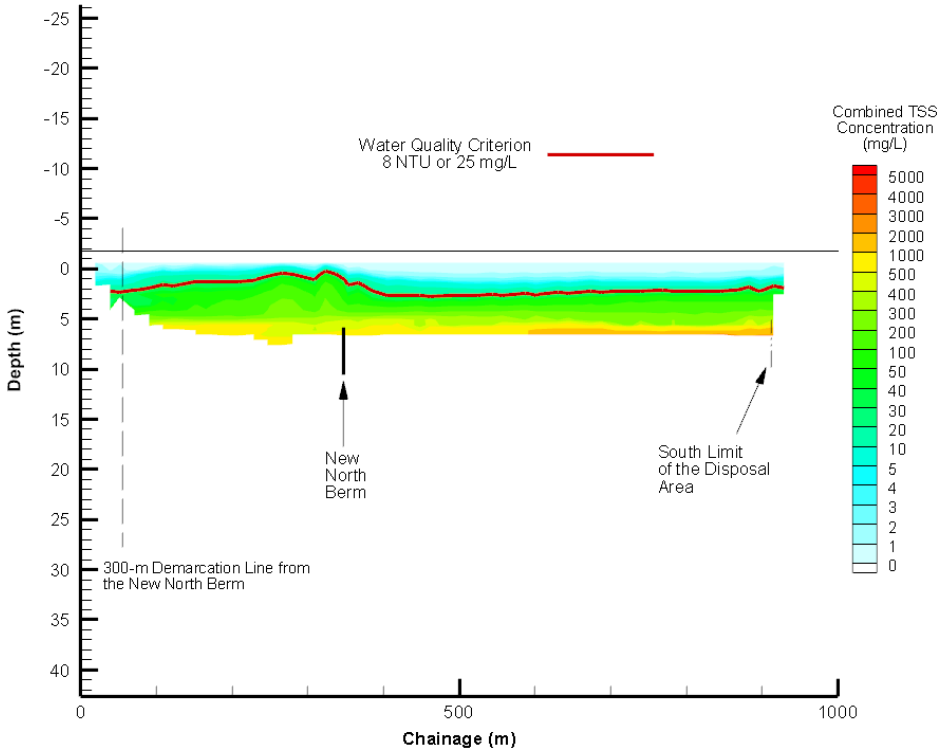

Figure 5.10 Northeast-Southwest Sectional Combined TSS Concentration in the Late Period (Columbia Dredger) – Flood Tide Approximately 3 hours before High Tide in December

The TSS concentration in the top 3-m of the water column increases in the later period with the Columbia dredger; this is expected due to the significant decrease of the water depth thus the decrease amount of available water for dilution of the dispersed TSS. Non-conformity with the water criterion value occurs, as shown in Figure 5.8, for a certain period of time, but the amount of time per day such non-conformity occurs will be discussed in Section 5.1.5 below.

5.1.4 Late Period – 309 (Scenario 4)

The snapshot of the TSS concentration, resulting from the 309 operation, on December 1, 8PM in the top 3-m is shown in plan view in Figure 5.11, and the corresponding sectional TSS profiles along the Northwest-Southeast and Northeast-Southwest lines are shown respectively in Figure 5.12 and Figure 5.13.

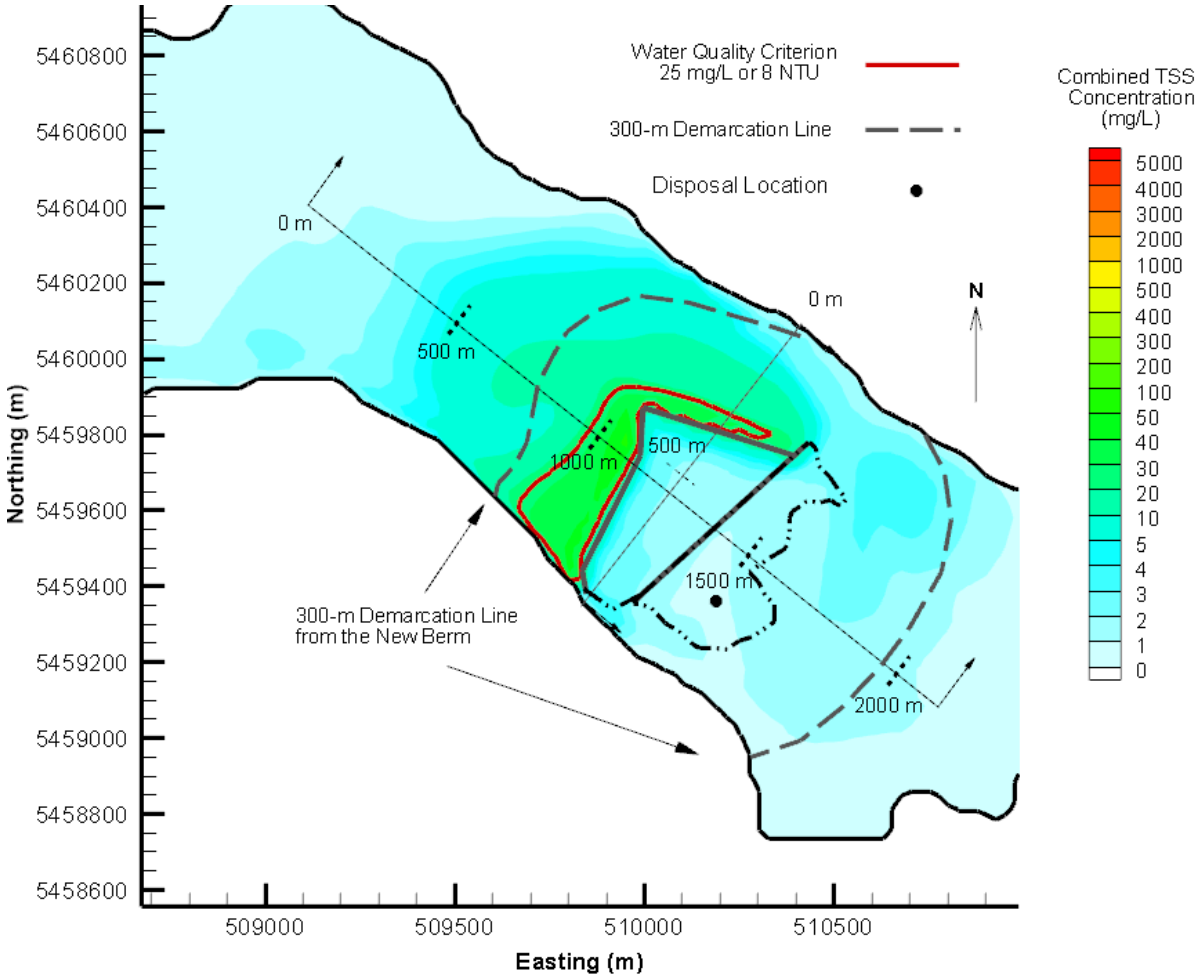

Figure 5.11 Combined TSS Concentration, Averaged between 0 m and 3 m Water Depth in the Late Period (309 Dredger) – Flood Tide Approximately 3 hours before High Tide in December

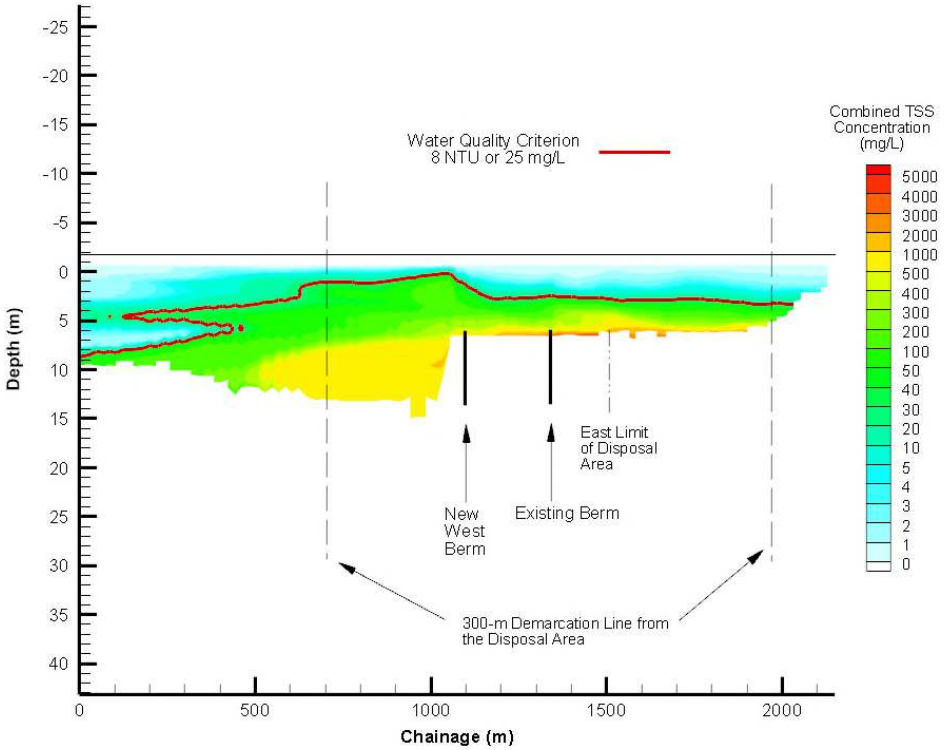

Figure 5.12 Northwest-Southeast Sectional Combined TSS Concentration in the Late Period (309 Dredger) – Flood Tide Approximately 3 hours before High Tide in December

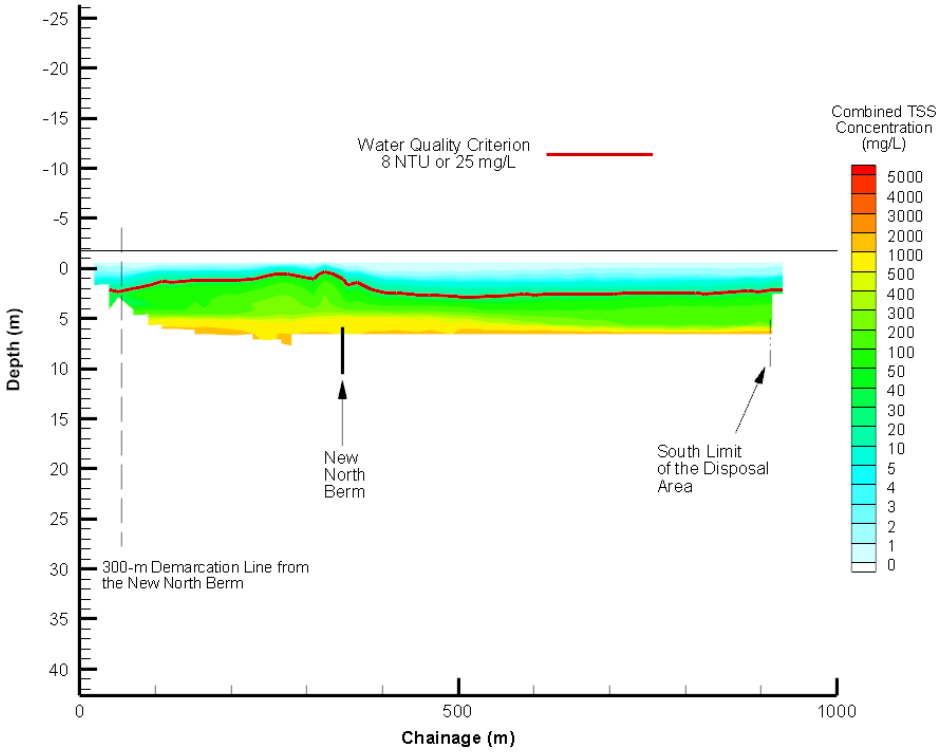

Figure 5.13 Northeast-Southwest Sectional Combined TSS Concentration in the Late Period (309 Dredger) – Flood Tide Approximately 3 hours before High Tide in December

Similar to the one with Columbia dredger, the operation with the 309 dredger displays similar augmentation of TSS concentration in the top 3-m of the water column. For a certain period of time, as shown in Figure 4.11, the criterion value for water quality is non-conformant for the top 3-m at the 300-m demarcation line. However, as presented in Section 4.1.5 below, the amount of time such non-conformity occurs is not significant. The dispersal operation with the Columbia generally lead to a lower TSS concentration due to its lower discharge rate of solids than the 309, even though the disposal period occupies 60% of the duty cycle for Columbia and only 20% for 309.

5.1.5 Statistical Results

The above section illustrates a snapshot of the so-called 'worst case' scenario when the combined TSS concentration reaches its highest value in the top 3-m. While it provides an indication of the upper bound concentration value one might expect during the dispersal operation, the results presented above represents the concentration at one point in time and certainly does not draw any conclusion on the pre-dominant TSS concentration in the water column over the course of the entire dispersal operation. Therefore, statistical analysis is undertaken for the combined TSS concentration, averaged over the top 3-m of the water column, at the 300-m demarcation line from the new berm for the operation in the early period when dredgeate is being dispersed in the main containment, and at the 300-m demarcation line from the existing berm for the operation in the late period when dispersal operation is in the existing containment.

To indicate the degree of conformity, in space and time, with the criterion TSS value, percentile modelled TSS concentration is an appropriate indicator. For example, the 90th percentile concentration is the concentration below which 90 percent of the TSS concentration values under consideration (i.e., along the 300-m limes, over the entire dredging operation) are found to lie. Table 4.1 below details the 90th, 95th and 100th percentile TSS concentration, averaged over the top 3 m of the water column, at the 300-m demarcation lines. Also included in the table is the corresponding NTU based on the factor of 3.13 derived from the equivalency of 25 mg/L to 8 NTU applied in the CCME guidelines.

Table 4.1 the Percentile TSS Concentration for the Top 3 m at the 300-m Demarcation Line

Dredger	90th Percentile		95th Percentile		100th Percentile or Maximum	
	Combined TSS Conc. (mg/L)	Equivalent NTU	Combined TSS Conc. (mg/L)	Equivalent NTU	Combined TSS Conc. (mg/L)	Equivalent NTU
Early Period						
Columbia	0.0137	0.0044	0.0281	0.0090	0.3866	0.1237
309	0.1389	0.0444	0.2621	0.0839	2.1499	0.6880
Late Period						
Columbia	3.6092	1.1549	5.1351	1.6432	21.0981	6.7514
309	4.1842	1.3389	6.0861	1.9476	22.8330	7.3066

The 90th percentile concentration indicates a general conformity of the TSS concentration for the top 3 m of the water column along the 300-m demarcation lines. In fact, the 95th percentile as well as the 100th percentile (or maximum) concentrations at the demarcation line are all under the criterion value

The model results also indicate that non-conformity with of the water quality criterion, if any, occurs in isolated patches along the demarcation lines, while TSS concentration in other sections along the lines remain well below the criterion value.

It is expected that as the depth at which the dredgeate is being dispersed becomes shallower, the amount of water available for dilution of the dispersed dredgeate decreases, thus the TSS concentration and the frequency of non-conformity of the water quality criterion increase.

Table 4.2 below shows the number of hours per day that the combined TSS concentration, averaged over the top 3-m, stays at or below the water quality criterion value of 25 mg/L (8 NTU) along the entire length of the demarcation lines. Also shown in the table is the corresponding number of hours per day of non-conformity to the criterion TSS value.

Table 4.2 The Number of Hours per Day for Conformity of TSS Concentration Criterion along the Entire 300-m Demarcation Line

Dredger	No of Hours per Day for TSS Concentration Conformity (hr)	No of Hours per Day for TSS Concentration Non-conformity (hr)
Early Period (Demarcation Line is 300-m from the West Berm)		
Columbia	24	~0
309	24	~0
Late Period (Demarcation Line is 300-m from the Existing Berm)		
Columbia	24	~0
309	24	~0

Table 4.2 suggests that, on a daily basis, there is negligible amount of time of TSS non-conformity. The criterion TSS concentration, according to the CCME guidelines, applies to the 24-hour exposure time, which means the operation will not lead to any non-conformity of the TSS criterion concentration when criterion exposure time is also included. In other words, the proposed disposal operation will not lead to any harmful, short-term exposure of aquatic life to the TSS as a result of the disposal operation.

6.0 CONCLUSION

The proposed dredge and disposal operation at the PCT site in Port Moody will involve placement of the dredgeate in the two containment basins: the new basin and the existing basin. The model study found that while a distinct density current will be formed as a result of the density difference between the ambient water and the dredgeate slurry that is being discharged at the diffuser terminus, fugitive, suspended sediment will inevitably be generated and be transported by the local circulation pattern to other part of the water body.

The resulting sediment plume, generated as a result of the fugitive solids, varies in shape and behaviour depending on the tidal stage and the location of the discharge terminus. The TSS concentration generally decreases with distance from the discharge point as the suspended dredgeate mixes with the cleaner ambient water in Port Moody Arm.

The model results show that the TSS concentration is generally higher towards the end of the operation when the containment cells, in which the dredgeate is being disposed, become shallower and when the amount of cleaner water available for mixing becomes less. Nonetheless, the combined TSS concentration, averaged over the top 3 m of the water column, generally conforms with the criterion value of 25 mg/L or 8 NTU at the 300-m demarcation line both in the early part and late part of the operation, and the disposal operation will not lead to harmful exposure of aquatic life to the TSS in the short term.

7.0 LIMITATIONS OF REPORT

This report and its contents are intended for the sole use Pacific Coast Terminal and their agents. Tetra Tech Canada Inc. does not accept any responsibility for the accuracy of any of the data, the analysis, or the recommendations contained or referenced in the report when the report is used or relied upon by any Party other than Pacific Coast Terminal, or for any Project other than the proposed development at the subject site. Any such unauthorized use of this report is at the sole risk of the user. Use of this document is subject to the Tetra Tech-Pacific Coast Terminal contract and the Limitations on the Use of this Document attached in Appendix B.

8.0 CLOSURE

We trust this technical memo meets your present requirements. If you have any questions or comments, please contact the undersigned.

Respectfully submitted,
Tetra Tech Canada Inc.

ISSUED FOR REVIEW

Prepared by:
Albert Leung, M.A.Sc., P.Eng., P.E.
Hydrotechnical Engineer
Water Practice
Direct Line: 778.945.5730
Albert.Leung@tetratech.com

ISSUED FOR REVIEW

Reviewed by:
Jim Stronach, Ph.D., P.Eng.
Physical Oceanographer
Manager, Water & Marine Engineering'
Water Practice
Direct Line: 778.945.5849
Jim.Stronach@tetratech.com

/

Attachments: Appendix A – H3D Technical Description
Appendix B – Tetra Tech's Limitations on the use of this Document

APPENDIX A

H3D TECHNICAL DESCRIPTION

APPENDIX A: H3D TECHNICAL DESCRIPTION

1.0 INTRODUCTION

H3D is an implementation of the numerical model developed by Backhaus (1983; 1985) which has had numerous applications to the European continental shelf, (Duwe et al., 1983; Backhaus and Meir Reimer, 1983), Arctic waters (Kampf and Backhaus, 1999; Backhaus and Kampf, 1999) and deep estuarine waters, (Stronach et al., 1993). Locally, H3D has been used to model the temperature structure of Okanagan Lake (Stronach et al., 2002), the transport of scalar contaminants in Okanagan Lake, (Wang and Stronach, 2005), sediment movement and scour / deposition in the Fraser River, circulation and wave propagation in Seymour and Capilano dams, and salinity movement in the lower Fraser River. H3D forms the basis of the model developed by Saucier and co-workers for the Gulf of St. Lawrence (Saucier et al., 2003), and has been applied to the Gulf of Mexico (Rego et al., 2010). H3D and its hydrocarbon transport and weathering module have been used in three recent environmental assessment applications currently before the appropriate regulatory agencies. H3D was used to simulate an existing and proposed reservoir for BC Hydro's Site C Clean Energy Project. Temperature, ice cover, and sedimentation characteristics of the proposed reservoir were predicted, supported by model validations in existing Dinosaur Reservoir. Two reports are available at the provincial Environmental Assessment Office. H3D was used to do oil spill modelling for the environmental and engineering assessments for the proposed Gateway project involving oil shipment out of Kitimat. The modelling work forms part of the information package submitted to the National Energy Board which is currently under review. Similarly, H3D was used to assess the fate of accidental fuel spills arising from a proposed jet fuel terminal in the Fraser River. This modelling work is part of the information package submitted to the provincial Environmental Assessment Office.

2.0 THEORETICAL BASIS

H3D is a three-dimensional time-stepping numerical model which computes the three components of velocity (u,v,w) on a regular grid in three dimensions (x,y,z), as well as scalar fields such as temperature and contaminant concentrations. The model uses the Arakawa C-grid (Arakawa and Lamb, 1977) in space, and uses a two level semi-implicit scheme in the time domain. H3D bears many similarities to the well-known Princeton Ocean Model (POM) (Blumberg and Mellor, 1987) in terms of the equations it solves, but differs in how the time-domain aspects are implemented. H3D uses a semi-implicit scheme, allowing relatively large time steps, and does not separately solve the internal and external models as POM does. It also uses a considerably simpler turbulence scheme in the vertical. These considerations combined allow H3D to execute complex problems relatively quickly.

The equations to be solved are:

Mass Conservation:

$$\frac{\partial u}{\partial x}+\frac{\partial v}{\partial y}+\frac{\partial w}{\partial z}=0 \tag{A1}$$

At the end of each timestep equation, (A1) is used to diagnostically determine the vertical component of velocity *(w)* once the two horizontal components of velocity (*u* and v) have been calculated by the model.

X-directed momentum:

$$\frac{\partial u}{\partial t}+u\frac{\partial u}{\partial x}+v\frac{\partial u}{\partial y}+w\frac{\partial u}{\partial z}+g\frac{\partial \eta}{\partial x}+\frac{1}{\rho_o}\frac{\partial}{\partial x}\int_z^\eta(\rho_w-\rho_o)gdz-fv-\frac{\partial}{\partial x}A_H\frac{\partial u}{\partial x}-\frac{\partial}{\partial y}A_H\frac{\partial u}{\partial y}-\frac{\partial}{\partial z}A_V\frac{\partial u}{\partial z}=0. \tag{A2}$$

Y-directed momentum:

$$\frac{\partial v}{\partial t}+u\frac{\partial v}{\partial x}+v\frac{\partial v}{\partial y}+w\frac{\partial v}{\partial z}+g\frac{\partial \eta}{\partial y}+\frac{1}{\rho_o}\frac{\partial}{\partial y}\int_z^\eta(\rho_w-\rho_o)gdz+fu-\frac{\partial}{\partial x}A_H\frac{\partial v}{\partial x}-\frac{\partial}{\partial y}A_H\frac{\partial v}{\partial y}-\frac{\partial}{\partial z}A_V\frac{\partial v}{\partial z}=0. \tag{A3}$$

Water surface elevation determined from the vertically-integrated continuity equation:

$$\frac{\partial \eta}{\partial t}=-\frac{\partial}{\partial x}\int_{-H}^{\eta}udz-\frac{\partial}{\partial y}\int_{-H}^{\eta}vdz. \tag{A4}$$

The effect of wind forcing introduced by means of the surface wind-stress boundary condition:

$$\left(A_V\frac{\partial u}{\partial z},A_V\frac{\partial v}{\partial z}\right)_{z=\eta}=\frac{\rho_a}{\rho_w}C_{D,air}\vec{U}_{wind}\left|\vec{U}_{wind}\right|. \tag{A5}$$

The effect of bottom friction introduced by the bottom boundary condition:

$$\left(A_V\frac{\partial u}{\partial z},A_V\frac{\partial v}{\partial z}\right)_{z=-H}=K_{bottom}\vec{U}_{bottom}\left|\vec{U}_{bottom}\right|. \tag{A6}$$

The bottom friction coefficient is usually understood to apply to currents at an elevation of one metre above the bottom. The bottom-most vector in H3D will, in general, be at a different elevation, i.e., at the midpoint of the lowest computational cell. H3D uses the 'law of the wall' to estimate the flow velocity at one metre above the bottom from the modelled near-bottom velocity.

The evolution of scalars, such as salinity, temperature, or suspended sediment, is given by the scalar transport/diffusion equation:

$$\frac{\partial S}{\partial t}+u\frac{\partial S}{\partial x}+v\frac{\partial S}{\partial y}+w\frac{\partial S}{\partial z}-\frac{\partial}{\partial x}N_H\frac{\partial S}{\partial x}-\frac{\partial}{\partial y}N_H\frac{\partial S}{\partial y}-\frac{\partial}{\partial z}N_V\frac{\partial S}{\partial z}=Q. \tag{A7}$$

In the above equations:

u(x,y,z,t): component of velocity in the *x* direction;

v(x,y,z,t): component of velocity in the *y* direction;

w(x,y,z,t): component of velocity in the *z* direction;

S(x,y,z,t): scalar concentration;

Q(x,y,z,t): source term for each scalar species

f: Coriolis parameter, determined by the earth's rotation and the local latitude;

$A_H\left(\partial u/\partial x, \partial u/\partial y, \partial v/\partial x, \partial v/\partial y\right)$: horizontal eddy viscosity;

$A_V\left(\partial u/\partial z, \partial v/\partial z, \partial \rho_{water}/\partial z\right)$: vertical eddy viscosity;

N_H: horizontal eddy diffusivity;

$N_V\left(\partial u/\partial z, \partial v/\partial z, \partial \rho_{water}/\partial z\right)$: vertical eddy diffusivity;

$C_{D,air}$: drag coefficient at the air-water interface;

$C_{D,bottom}$: drag coefficient at the water/sea bottom interface;

ρ_a: density of air;

$\rho_w(x,y,z,t)$: density of water;

ρ_o : reference density of water;

$\eta(x,y,t)$: water surface elevation;

H(x,y) : local depth of water.

The above equations are formally integrated over the small volumes defined by the computational grid, and a set of algebraic equations results, for which an appropriate time-stepping methodology must be found. Backhaus (1983, 1985) presents such a procedure, referred to as a semi-implicit method. The spatially-discretized version of the continuity equation is written as:

$$\eta^{(1)} = \eta^{(0)} - \alpha\frac{\Delta t}{\Delta l}(\delta_x U^{(1)} + \delta_y V^{(1)}) - (1-\alpha)\frac{\Delta t}{\Delta l}(\delta_x U^{(0)} + \delta_y V^{(0)}) \qquad \text{(A8)}$$

where superscript *(0)* and *(1)* refer to the present and the advanced time, δ_x and δ_y are spatial differencing operators, and *U* and *V* are vertically integrated velocities. The factor α represents an implicit weighting, which must be greater than 0.5 for numerical stability. $U^{(0)}$ and $V^{(0)}$ are known at the start of each computational cycle. $U^{(1)}$, and similarly $V^{(1)}$, can be expressed as:

$$U^{(1)} = U^{(0)} - g\alpha\Delta t\eta_x^{(1)} - g(1-\alpha)\Delta t\eta_x^{(0)} + \Delta t X^{(0)} \qquad \text{(A9)}$$

where $X^{(0)}$ symbolically represents all other terms in the equation of motion for the u- or v-component, which are evaluated at time level *(0)*: Coriolis force, internal pressure gradients, non-linear terms, and top and bottom stresses,*)*. When these expressions are substituted into the continuity equation (A4), after some further manipulations, there results an elliptic equation for $\delta_{i,k}$, the change in water level over one timestep at grid cell *i,k* (respectively the *y* and *x* directions):

$$\delta_{i,k} - (ce\delta_{i,k+1} + cw\delta_{i,k-1} + cn\delta_{i-1,k} + cs\delta_{i+1,k}) = Z_{i,k} \quad \text{(A10)}$$

where *ce*, *cw*, *cn*, and *cs* are coefficients depending on local depths and the weighting factor (α), and $Z_{i,k}$ represents the sum of the divergence formed from velocities at time level *(0)* plus a weighted sum of adjacent water levels at time level *(0).*

Once equation (A10) is solved for $\delta_{i,k}$, the water level can be updated:

$$\eta_{i,k}^{(1)} = \eta_{i,k}^{(0)} + \delta_{i,k} \quad \text{(A11)}$$

and equation (A9) can be completed.

At the end of each timestep, volume conservation is used to diagnostically compute the vertical velocity *w(j,i,k)* from the two horizontal components *u* and *v*.

2.1 Vertical Grid Geometry

In the vertical, the levels near the surface are typically closely spaced to assist with resolving near-surface dynamics. In addition, the model is capable of dealing with relatively large excursions in overall water level as the water level rises and falls in response to varying inflows and outflows, by allowing the number of near-surface layers to change as the water level varies. That is, as water levels rise in a particular cell, successive layers above the original layer are turned on and become part of the computational mesh. Similarly, as water levels fall, layers are turned off. This procedure has proven to be quite robust, and allows for any reasonable vertical resolution in near-surface waters. When modelling thin river plumes in areas of large tidal range, the variable number of layers approach allows for much better control over vertical resolution than does the σ-coordinate method.

In addition to tides, the model is able to capture the important response, in terms of enhanced currents and vertical mixing, to wind-driven events. This is achieved by applying wind stress to each surface grid point on each time step. Vertical mixing in the model then re-distributes this horizontal momentum throughout the water column. Similarly, heat flux through the water surface is re-distributed by turbulence and currents in temperature simulations.

2.2 Turbulence Closure

Turbulence modelling is important in determining the correct distribution of velocity and scalars in the model. The diffusion coefficients for momentum (A_H and A_V) and scalars (N_H and N_V) at each computational cell are dependent on the level of turbulence at that point. H3D uses a shear-dependent turbulence formulation in the horizontal, (Smagorinsky, 1963). The basic form is:

$$A_H = A_{Ho}\, dx\, dy \sqrt{\left(\frac{du}{dx}\right)^2 + \left(\frac{dv}{dy}\right)^2 + \frac{1}{2}\left(\frac{\partial v}{\partial x} + \frac{\partial u}{\partial y}\right)^2} \quad \text{(A12)}$$

The parameter A_{H0} is a dimensionless tuning variable, and experience has shown it to lie in the range of 0.25 to 0.45 for most water bodies such as rivers, lakes and estuaries.

A shear and stratification dependent formulation, the Level 2 model of Mellor and Yamada (1982), is used for the vertical eddy diffusivity. The basic theory for the vertical viscosity formulation is taken from an early paper, Mellor and Durbin (1975). The evaluation of length scale is based on a methodology presented in Mellor and Yamada (1982).

For scalars, both horizontal and vertical eddy diffusivity are taken to be similar to their eddy viscosity counterparts, but scaled by a fixed ratio from the eddy viscosity values. Different ratios are used for the horizontal and vertical diffusivities. If data is available for calibration, these ratios can be adjusted based on comparisons between modelled and observed data. Otherwise, standard values based on experience with similar previously modelled water bodies are used. In a recent reservoir simulation, the ratio of vertical eddy diffusivity to vertical eddy viscosity was 0.75 and the ratio between horizontal eddy diffusivity and horizontal eddy viscosity was 1.0.

2.3 Scalar Transport

The scalar transport equation implements a form of the flux-corrected algorithm (Zalesak, 1979), in which all fluxes through the sides of each computational cell are first calculated using a second-order method. Although generally more accurate than a first order method, second order flux calculations can sometimes lead to unwanted high frequency oscillations in the numerical solution. To determine if such a situation is developing, the model examines each cell to see if the computed second order flux would cause a local minimum or maximum to develop. If so, then all fluxes into or out of that cell are replaced by first order fluxes, and the calculation is completed. As noted, the method is not a strict implementation of the Zalesak method, but is much faster and achieves very good performance with respect to propagation of a Gaussian distribution through a computational mesh. It does not propagate box-car distributions as well as the full Zalesak method, but achieves realistic simulations of the advection of scalars in lakes, rivers and estuaries, which is the goal of the model. This scheme as implemented is thus a good tradeoff between precision and execution time, important since in many situations, where more than one scalar is involved, the transport-diffusion algorithm can take up more than half the execution time.

2.4 Heat Flux at the Air-Water Interface

The contribution of heat flux to the evolution of the water temperature field can be schematized as:

$$\frac{dT}{dt} = \frac{\Delta Q}{\rho * c_p * h}$$

where ΔQ is the net heat flux per unit area retained in a particular layer, ρ is the density of water, c_p is the heat capacity of water and h is the layer thickness.

Heat flux at the air-water interface incorporates the following terms:

Q_{in}: incident short wave radiation. Generally, this is not known from direct observations. Generally, it is estimated from the cloud cover and opacity observations at nearby stations, a theoretical calculation of radiation at the top of the atmosphere based on the geometry of the earth/sun system, and an empirical adjustment based on radiation measurements at Vancouver Airport and UBC respectively for the period 1974-1977. This procedure has worked well for many water bodies, notably Okanagan Lake and the waters of

the north coast of British Columbia, in terms of allowing H3D to reproduce the observed temperature distributions in space and time. Values for albedo as a function of solar height are taken from Kondratyev (1972).

Q_{back}: net long wave radiation, calculated according to Gill (1982), involving the usual fourth power dependence on temperature, a factor of 0.985 to allow for the non-black body behaviour of the ocean, a factor depending on vapor pressure to allow for losses due to back radiation from moisture in the air, and a factor representing backscatter from clouds.

Q_L and Q_H: latent and sensible heat flux. Latent heat flux (Q_L) is the heat carried away by the process of evaporation of water. Sensible heat flux (Q_S) is driven by the air-water temperature difference and is similar to conduction, but assisted by turbulence in the air. Latent and sensible heat flux is described by:

$$Q_L = 1.32e^{-3} * L * windspeed * (q_{obs} - q_{sat}) * latent\_factor$$

$$Q_S = 1.46e^{-3} * \rho_{air} * c_p * windspeed * (T_{air} - T_{water}) * sensible\_factor$$

Where q_{obs} and q_{sat} are the observed and saturated specific humidities, T_{air} and T_{water} are the air and water temperatures, L is the latent heat of evaporation of water, and c_p is the heat capacity of water. '*latent_factor*' and '*sensible_factor*' are scaling factors introduced to account for local factors, and can be adjusted, when needed, to achieve better calibration of the model. Typically, the only adjustment is that *Sensible_factor* is doubled when the air temperature is less than the water or ice surface temperature to account for increased turbulence in an unstable air column.

Light absorption in the water column. As light passes through the water column it is absorbed and the absorbed energy is a component of the energy balance that drives water temperature. H3D assumes that light attenuation follows an exponential decay law:

$$E(z) = E(z_0) * e^{-k*(z-z_0)}$$

The model computes the energy at the top and bottom of each layer and the difference is applied to the general heat equation in that layer. The extinction coefficient (k) is related to the Secci depth (D_s) by

$$k = \frac{2.1}{D_s}$$

Temperature is treated like any other scalar as far as advection and diffusion are concerned. Heat flux at the water-sediment interface is not currently included in H3D.

2.5 Ice

The ice model is generally based on processes described in Patterson and Hamblin (1988). The ice cover is characterized by a thickness, a fraction of the cell covered, and an ice surface temperature. The temperature of the bottom of the ice is assumed to be the temperature of melting, usually 0º C. The strategy is to compute the differences in heat flux at the top and bottom of the ice layer and use this difference to determine the growth or decay rate and the change in temperature of the ice. The heat flux at

the bottom of the ice layer is dependent on lake temperature and water velocity. The heat flux at the top is dependent on meteorological processes and the surface temperature of the ice. The surface heat flux to the top of the ice sheet is calculated in a similar way as for open water, except that latent heat flux term (Q_L) also includes the heat of fusion. Albedo is also altered to account for ice/snow cover.

In order to start ice formation, once the surface water temperature drops below 3º C in a particular cell, a test ice layer of thickness 1 cm is initialized. If the test thickness melts in one time step, then the system cannot support ice cover in that cell at that time. If it survives, then the amount of ice in that cell is converted to a 1 cm thick region with coverage calculated from the mass of ice formed. In this way, a relatively robust start is made to ice formation.

The frictional interaction between the bottom of the ice and the immediately adjacent water is parameterized according to Nezhikhovskiy (1964).

2.6 Validation

Three validations of H3D's water level and temperature prediction skill are discussed below.

2.6.1 Strait of Georgia/Point Atkinson Tide: Wave Propagation

A fundamental concern with a circulation model such as H3D is how well it propagates waves, the carriers of information through the system. Figure A-1 presents results of a simulation of tides in the Strait of Georgia and Juan de Fuca Strait, with tidal elevations prescribed at the entrance to Juan de Fuca Strait and at a section north of Texada Island in the Strait of Georgia. The complex dynamics of the northern passes, such as Discovery Passage and Seymour Narrows, are thus avoided, allowing a test of H3D's wave propagation capabilities. The figure plots the modelled water level at Point Atkinson in red, and the observed water level in black. There is nearly perfect agreement, with the slight difference resulting from small storm surge events. This validation demonstrates that the selection of grid schematization (Arakawa C-grid) and the semi-implicit time-stepping approach have produced a system than can accurately propagate information through a water body.

2.6.2 Okanagan Lake Temperature Profiles

Obtaining good reproduction of the seasonally–evolving temperate structure of a lake indicates that the heat flux across the air-water interface is accurately parameterized and that the transport-diffusive processes operating in the water column are also accurately reproduced by the model. Figure A-2 presents a comparison of observed and computed temperature profiles at the northern end of Okanagan Lake near Vernon, in April, August, October and December of 1997. The agreement is very good as the model reproduced the transition from a well-mixed condition in the spring to the development of a strong thermocline in the summer, the deepening of the upper layer during the fall cooling period, and a return to isothermal conditions in winter. There is little doubt that H3D can compute accurate temperature distributions in water bodies, as long as adequate meteorological data is available. For this simulation, the meteorological data was obtained from Penticton Airport: winds, rotated to follow the thalweg of the valley; cloud cover, air temperature and relative humidity.

2.6.3 Thermistor Response: Okanagan Lake

Okanagan Lake is subject to significant fluctuations in the vertical thermal structure during the summer stratified period. Figure A-3 shows a temperature time-series at a site on the north side of the William R. Bennett Bridge which exhibits significant temperature excursions at periods of about 60 hours, or 2.5 days. Figure A-4 shows the modelled time series of temperature at three selected depths, 51 m, 21 m and 9 m. The occurrence and magnitude of the temperature fluctuations is generally predicted by the model, but the reproduction is not perfect: the occurrence and timing of the temperature events is quite good, but the modelled peaks appear to be generally somewhat broader in time. It was found that there were considerable differences in the simulated behaviour depending on whether winds at Kelowna Airport, which is situated in a side-valley, were included in the model or not. It is also clear that H3D can generally reproduce internal seiches in a lake, as long as adequate spatial resolution is used. This is particularly apparent when the coherent internal waves that propagate up and down the lake are examined in a longitudinal section, illustrated in two snapshots from a model simulation of such an event in Figure A-5.

REFERENCES

Arakawa, A. and V.R. Lamb. 1977. Computational design of the basic dynamical processes of the UCLA general circulation model. Methods in Computational Physics, 17, 173-263.

Backhaus, J.O. 1983. A semi-implicit scheme for the shallow water equations for applications to shelf sea modelling. Continental Shelf Research, 2, 243-254.

Backhaus, J.O. and E. Meir-Reimer. 1983. On seasonal circulation patterns in the North Sea. In: North Sea Dynamics, J. Sundermann and W. Lenz, editors. Springerr-Verlag, Heidelberg, pp 63-84.

Backhaus, J.O., and J. Kampf, 1999. Simulation of sub-mesoscale oceanic convection and ice-ocean interactions in the Greenland Sea. Deep Sea Research Part II: Topical Studies in Oceanography, 46, 1427-1455.

Backhaus, J.O., 1985. A three-dimensional model for the simulation of shelf-sea dynamics. Deutsche Hydrographische Zeitschrift, 38, 165-187.

Blumberg, A. F. and G. L. Mellor, A description of a three-dimensional coastal ocean circulation model, In Three-Dimensional Coastal Ocean Models, N. S. Heaps, editor. American Geophysical Union, Washington, DC, 1987, pp 1-16.

Duwe, K.C., R.R. Hewer, and J.O. Backhaus. 1983. Results of a semi-implicit two-step method for the simulation of markedly non-linear flow in coastal seas. Continental Shelf Research, 2, 255-274.

Friehe C.A. and K.F. Schmitt,1976. Parameterization of air-sea interface fluxes of sensible heat and moisture by the bulk aerodynamic formulas. Journal of Physical Oceanography. 76:801-805.

Kampf, J. and J.O Backhaus, 1999. Ice-ocean interactions during shallow convection under conditions of steady winds: three-dimensional numerical studies. Deep Sea Research Part II: Topical Studies in Oceanography, 46, 1335-1355.

Kondratyev, K.Y., 1972. Radiation Processes in the Atmosphere, WMO No. 309,.

Mellor, G.L. and P.A. Durbin. 1975. The structure and dynamics of the ocean surface mixed layer. Journal of Physical Oceanography, 5, 718-728.

Mellor, G.L. and T. Yamada. 1982. Development of a turbulence closure model for geophysical fluid problems. Reviews of Geophysics and Space Physics, 20, 851-875.

Nezhikhovskiy, R.A. 1964. Coefficients of roughness of bottom surface of slush-ice cover. Soviet Hydrology: Selected Papers, 2, 127-150.

Rego, J.L., E. Meselhe, J. Stronach and E. Habib. Numerical Modeling of the Mississippi-Atchafalaya Rivers' Sediment Transport and Fate: Considerations for Diversion Scenarios. Journal of Coastal Research, 26, 212-229.

Saucier, F.J.; F. Roy, D. Gilbert, P. Pellerin and H. Ritchie. 2003. The formationof water masses and sea ice in the Gulf of St. Lawrence. Journal of Geophysical Research, 108 (C8): 3269–3289.

Smagorinsky, J. 1963. General circulation experiments with primitive equations I. The basic experiment. Monthly Weather Review, 91, 91-164.

Stronach, J.A., J.O. Backhaus, and T.S. Murty. 1993. An update on the numerical simulation of oceanographic processes in the waters between Vancouver Island and the mainland: the G8 model. Oceanography and Marine Biology: an Annual Review, 31, 1-86.

Stronach, J.A., R.P. Mulligan, H. Soderholm, R. Draho, D Degen. 2002. Okanagan Lake Limnology: Helping to Improve Water Quality and Safety. Innovation, Journal of the Association of Professional Engineers and Geoscientists of B.C. November 2002.

Wang, E and J.A. Stronach. 2005. Summerland Water Intake Feasibility Study. In "Water – Our Limiting Resource", Proceedings of a conference held in Kelowna Feb 23-25, 2005. BC Branch, Canadian Water Resources Association. pp. 256 – 269.

Zalesak, S.T. 1979. Fully multidimensional flux-corrected transport algorithms for fluids. Journal of Computational Physics, 31, 335-362.

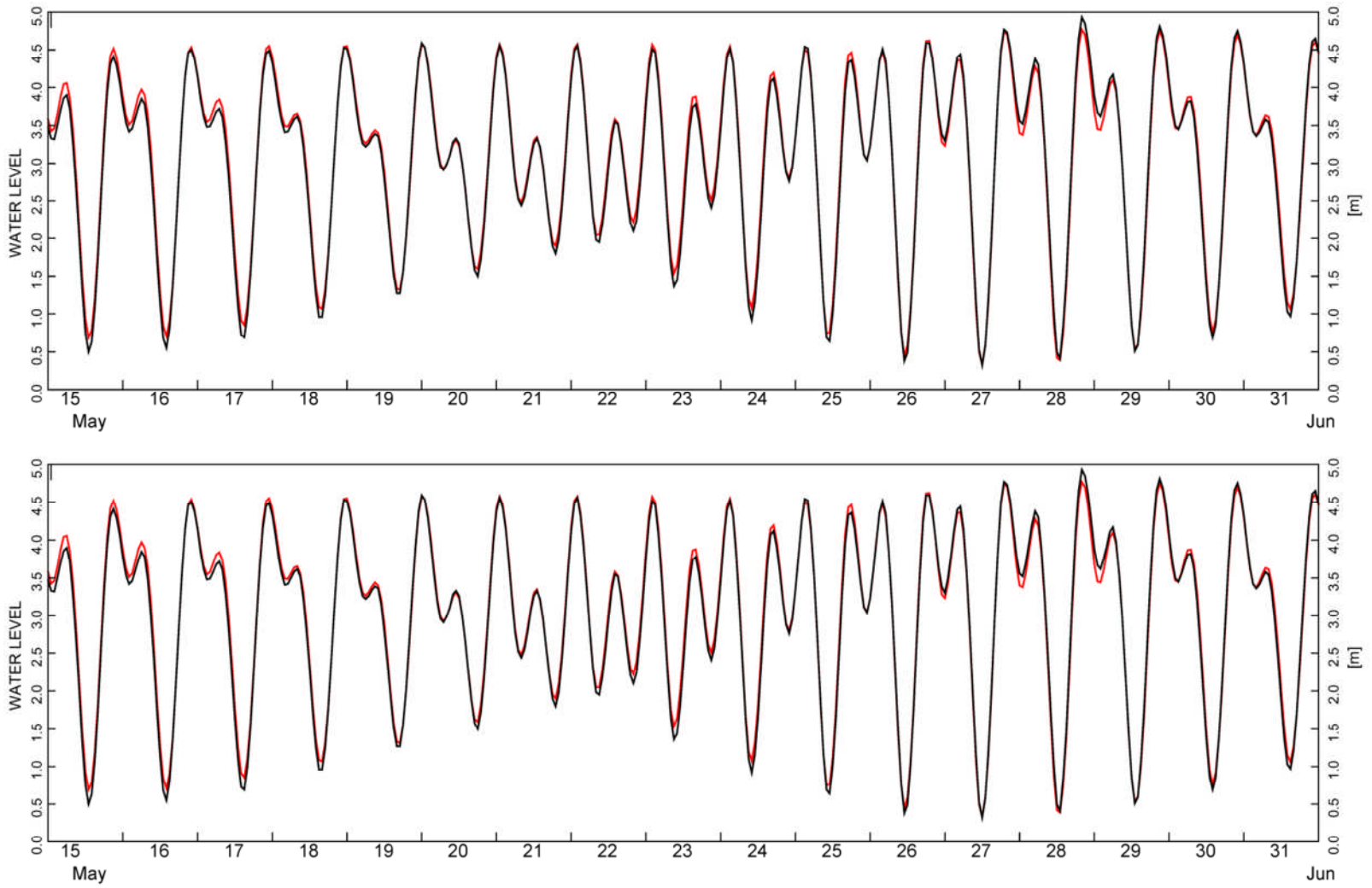

LEGEND

- Solid lines represent observed profiles
- Dash lines represent modelled profiles

NOTES

STATUS

CLIENT

-

H3D TECHNICAL DESCRIPTION

H3D Validation
Tidal Reproduction

eba
A TETRA TECH COMPANY

PROJECT NO.	DWN	CKD	APVD	REV
V132	AL	JAS	JAS	001

OFFICE	DATE
EBA-VANC	August 2011

Figure A-1

L:\src\H3D\Documentation\Tech Description 2013\Figures\FigureA1.docx

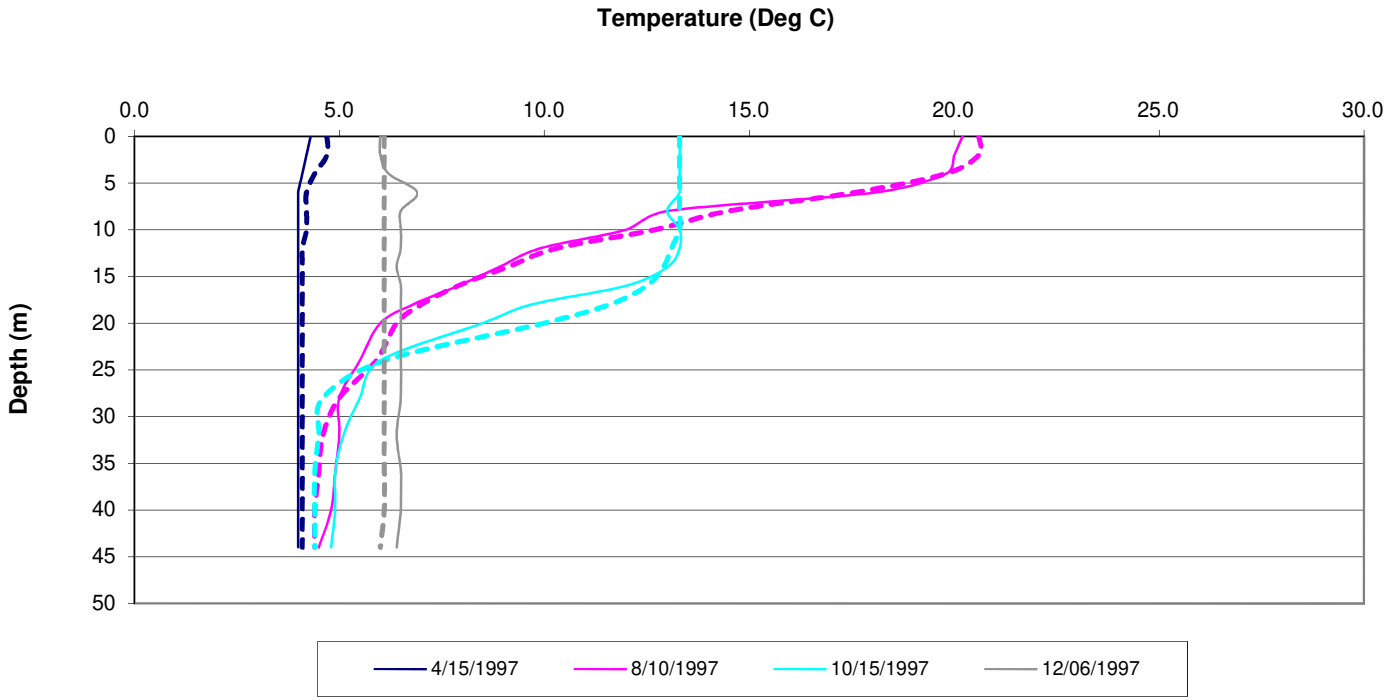

LEGEND

- Solid lines represent observed profiles
- Dash lines represent modelled profiles

NOTES

STATUS

CLIENT

-

H3D TECHNICAL DESCRIPTION

H3D Validation
Comparison of Observed and Modelled Temperature Profiles at Vernon

A TETRA TECH COMPANY

PROJECT NO.	DWN	CKD	APVD	REV
V132	AL	JAS	JAS	001

OFFICE	DATE
EBA-VANC	August , 2011

Figure A-2

L:\src\H3D\Documentation\Tech Description 2013\Figures\FigureA2.docx

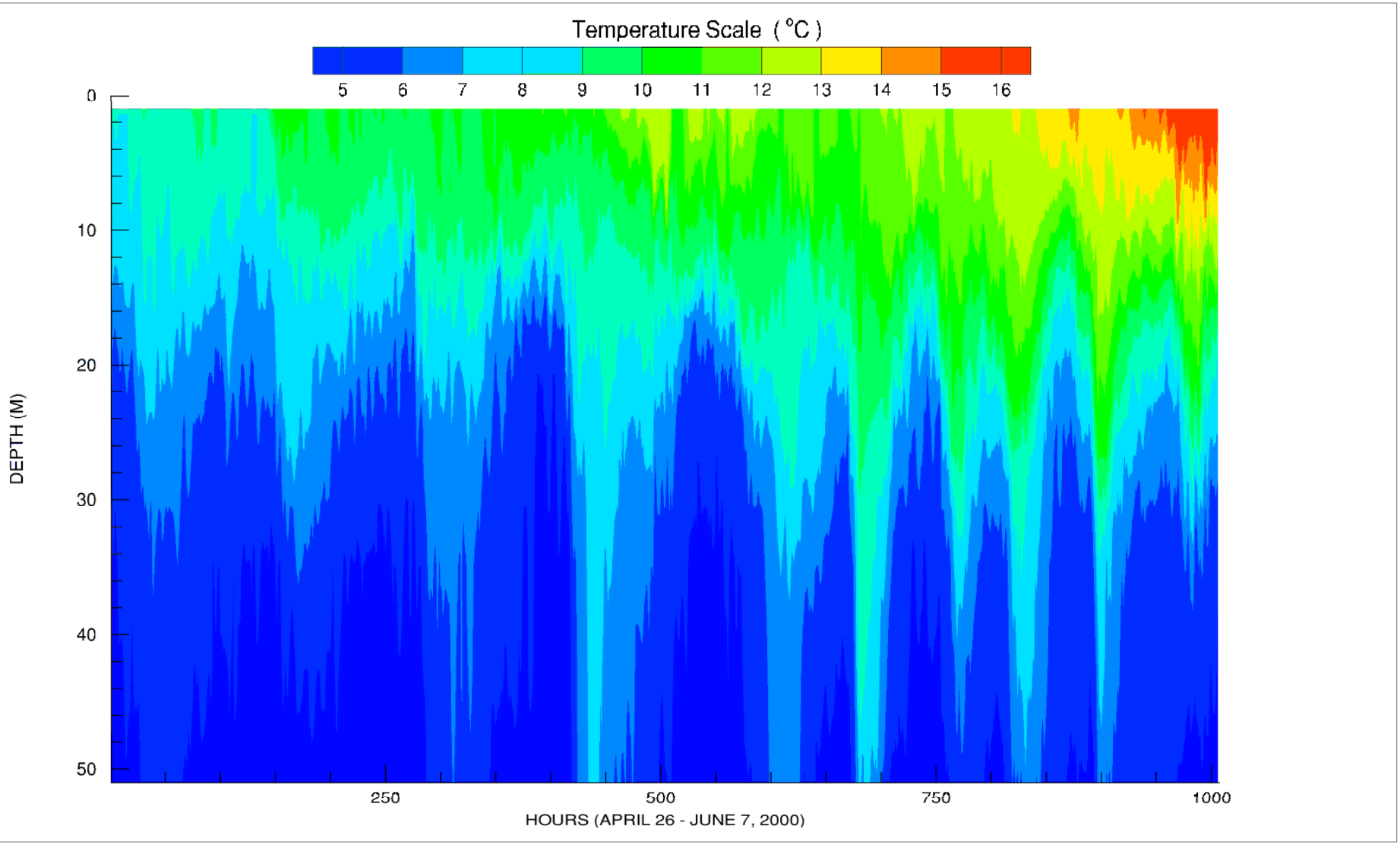

LEGEND

NOTES

CLIENT

-

STATUS
ISSUED FOR REVIEW

A TETRA TECH COMPANY

H3D TECHNICAL DESCRIPTION

H3D VALIDATION
SEICHES IN OKANAGAN LAKE
(OBSERVED DATA)

PROJECT NO.	DWN	CKD	APVD	REV
V132	EW	JAS	JAS	0

OFFICE	DATE
EBA-VANC	August 2, 2011

Figure A-3

L:\src\H3D\Documentation\Tech Description 2013\Figures\figureA3.doc

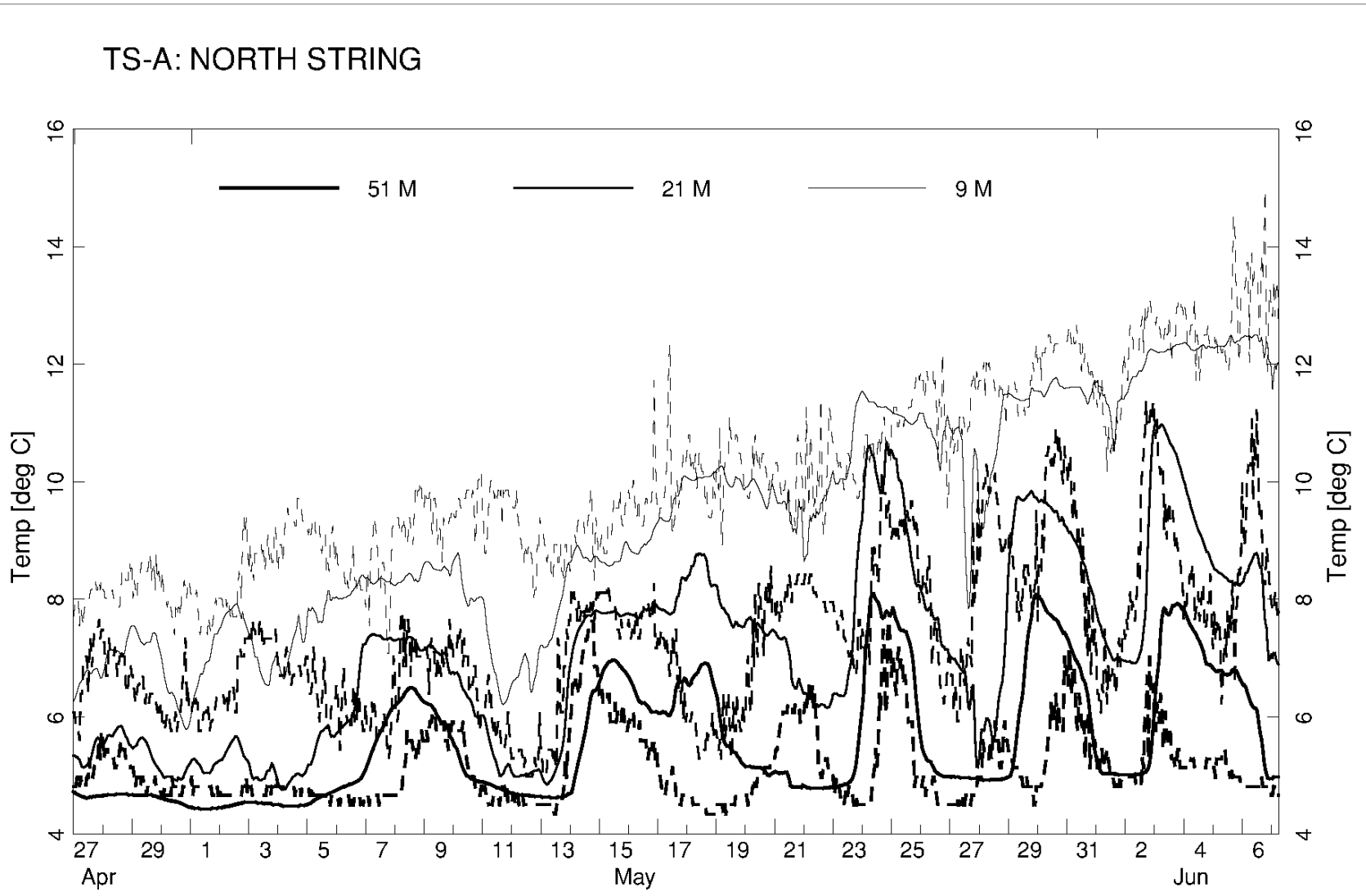

LEGEND

Dashed Lines: Observed Temperature
Solid Lines: Modelled Temperature

NOTES

STATUS
ISSUED FOR REVIEW

CLIENT
-

H3D TECHNICAL DESCRIPTION

H3D VALIDATION
INTERNAL SEICHE DYNAMICS
OKANAGAN LAKE

PROJECT NO.	DWN	CKD	APVD	REV
V132	EW	JAS	JAS	0

OFFICE	DATE
EBA-VANC	August 2, 2011

A TETRA TECH COMPANY

Figure A-4

L:\src\H3D\Documentation\Tech Description 2013\Figures\figureA4.doc

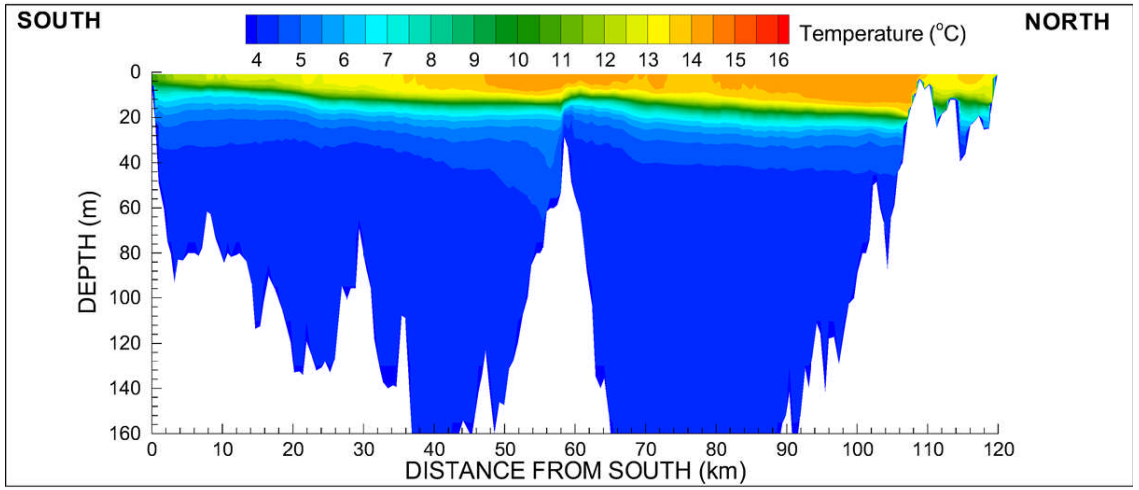

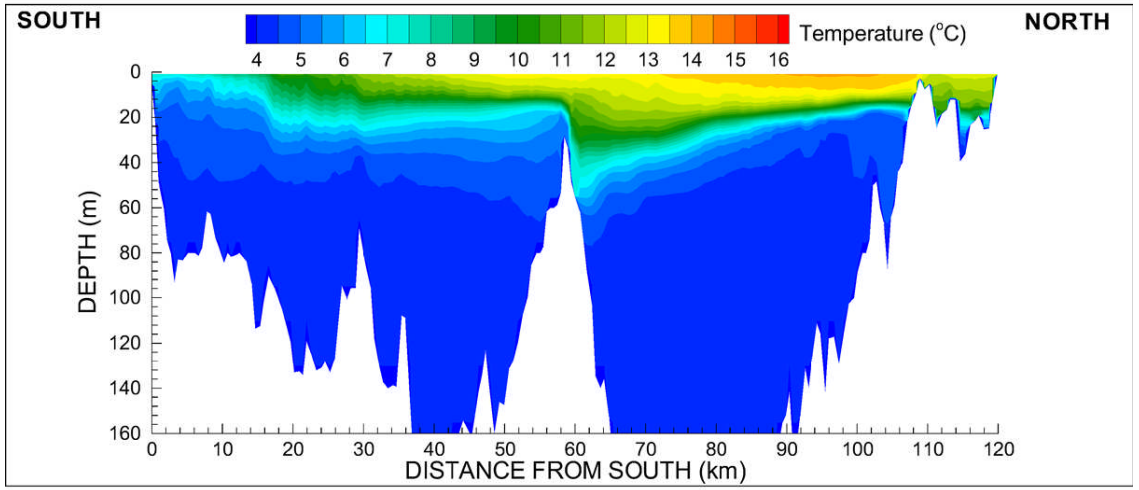

LEGEND

NOTES

STATUS
ISSUED FOR REVIEW

CLIENT
-

A TETRA TECH COMPANY

H3D TECHNICAL DESCRIPTION

H3D VALIDATION
INTERNAL SEICHE DYNAMICS
OKANAGAN LAKE

PROJECT NO.	DWN	CKD	APVD	REV
V132	EW	JAS	JAS	JAS

OFFICE	DATE
EBA-VANC	August 2, 2011

Figure A-5

L:\src\H3D\Documentation\Tech Description 2013\Figures\figureA5.doc

APPENDIX B

TETRA TECH'S LIMITATIONS ON THE USE OF THIS DOCUMENT

GENERAL CONDITIONS

HYDROTECHNICAL

This report incorporates and is subject to these "General Conditions".

1.0 USE OF REPORTS AND OWNERSHIP

This report pertains to a specific site, a specific development, and a specific scope of work. The report may include plans, drawings, profiles and other supporting documents that collectively constitute the report (the "Report").

The Report is intended for the sole use of Tetra Tech EBA's Client (the "Client") as specifically identified in the Tetra Tech EBA Services Agreement or other Contract entered into with the Client (either of which is termed the "Services Agreement" herein). Tetra Tech EBA does not accept any responsibility for the accuracy of any of the data, analyses, recommendations or other contents of the Report when it is used or relied upon by any party other than the Client, unless authorized in writing by Tetra Tech EBA.

Any unauthorized use of the Report is at the sole risk of the user. Tetra Tech EBA accepts no responsibility whatsoever for any loss or damage where such loss or damage is alleged to be or, is in fact, caused by the unauthorized use of the Report.

Where Tetra Tech EBA has expressly authorized the use of the Report by a third party (an "Authorized Party"), consideration for such authorization is the Authorized Party's acceptance of these General Conditions as well as any limitations on liability contained in the Services Agreement with the Client (all of which is collectively termed the "Limitations on Liability"). The Authorized Party should carefully review both these General Conditions and the Services Agreement prior to making any use of the Report. Any use made of the Report by an Authorized Party constitutes the Authorized Party's express acceptance of, and agreement to, the Limitations on Liability.

The Report and any other form or type of data or documents generated by Tetra Tech EBA during the performance of the work are Tetra Tech EBA's professional work product and shall remain the copyright property of Tetra Tech EBA.

The Report is subject to copyright and shall not be reproduced either wholly or in part without the prior, written permission of Tetra Tech EBA. Additional copies of the Report, if required, may be obtained upon request.

2.0 ALTERNATIVE REPORT FORMAT

Where Tetra Tech EBA submits both electronic file and hard copy versions of the Report or any drawings or other project-related documents and deliverables (collectively termed Tetra Tech EBA's "Instruments of Professional Service"), only the signed and/or sealed versions shall be considered final. The original signed and/or sealed version archived by Tetra Tech EBA shall be deemed to be the original. Tetra Tech EBA will archive the original signed and/or sealed version for a maximum period of 10 years.

Both electronic file and hard copy versions of Tetra Tech EBA's Instruments of Professional Service shall not, under any circumstances, be altered by any party except Tetra Tech EBA. Tetra Tech EBA's Instruments of Professional Service will be used only and exactly as submitted by Tetra Tech EBA.

Electronic files submitted by Tetra Tech EBA have been prepared and submitted using specific software and hardware systems. Tetra Tech EBA makes no representation about the compatibility of these files with the Client's current or future software and hardware systems.

3.0 STANDARD OF CARE

Services performed by Tetra Tech EBA for the Report have been conducted in accordance with the Services Agreement, in a manner consistent with the level of skill ordinarily exercised by members of the profession currently practicing under similar conditions in the jurisdiction in which the services are provided. Professional judgment has been applied in developing the conclusions and/or recommendations provided in this Report. No warranty or guarantee, express or implied, is made concerning the test results, comments, recommendations, or any other portion of the Report.

If any error or omission is detected by the Client or an Authorized Party, the error or omission must be immediately brought to the attention of Tetra Tech EBA.

4.0 ENVIRONMENTAL AND REGULATORY ISSUES

Unless expressly agreed to in the Services Agreement, Tetra Tech EBA was not retained to investigate, address or consider, and has not investigated, addressed or considered any environmental or regulatory issues associated with the project.

5.0 DISCLOSURE OF INFORMATION BY CLIENT

The Client acknowledges that it has fully cooperated with Tetra Tech EBA with respect to the provision of all available information on the past, present, and proposed conditions on the site, including historical information respecting the use of the site. The Client further acknowledges that in order for Tetra Tech EBA to properly provide the services contracted for in the Services Agreement, Tetra Tech EBA has relied upon the Client with respect to both the full disclosure and accuracy of any such information.

6.0 INFORMATION PROVIDED TO TETRA TECH EBA BY OTHERS

During the performance of the work and the preparation of this Report, Tetra Tech EBA may have relied on information provided by persons other than the Client.

While Tetra Tech EBA endeavours to verify the accuracy of such information, Tetra Tech EBA accepts no responsibility for the accuracy or the reliability of such information even where inaccurate or unreliable information impacts any recommendations, design or other deliverables and causes the Client or an Authorized Party loss or damage.

7.0 GENERAL LIMITATIONS OF REPORT

This Report is based solely on the conditions present and the data available to Tetra Tech EBA at the time the Report was prepared.

The Client, and any Authorized Party, acknowledges that the Report is based on limited data and that the conclusions, opinions, and recommendations contained in the Report are the result of the application of professional judgment to such limited data.

The Report is not applicable to any other sites, nor should it be relied upon for types of development other than those to which it refers. Any variation from the site conditions present at or the development proposed as of the date of the Report requires a supplementary investigation and assessment.

It is incumbent upon the Client and any Authorized Party, to be knowledgeable of the level of risk that has been incorporated into the project design, in consideration of the level of the hydrotechnical information that was reasonably acquired to facilitate completion of the design.

The Client acknowledges that Tetra Tech EBA is neither qualified to, nor is it making, any recommendations with respect to the purchase, sale, investment or development of the property, the decisions on which are the sole responsibility of the Client.

8.0 JOB SITE SAFETY

Tetra Tech EBA is only responsible for the activities of its employees on the job site and was not and will not be responsible for the supervision of any other persons whatsoever. The presence of Tetra Tech EBA personnel on site shall not be construed in any way to relieve the Client or any other persons on site from their responsibility for job site safety.